ORIGINAL PAPER

Calibration of the process-based model 3-PG for major central European tree species

David I. Forrester[1] ⬤ · Martina L. Hobi[1] · Amanda S. Mathys[1] · Golo Stadelmann[1] · Volodymyr Trotsiuk[1,2,3]

Abstract

Process-based forest models are important tools for predicting forest growth and their vulnerability to factors such as climate change or responses to management. One of the most widely used stand-level process-based models is the 3-PG model (Physiological Processes Predicting Growth), which is used for applications including estimating wood production, carbon budgets, water balance and susceptibility to climate change. Few 3-PG parameter sets are available for central European species and even fewer are appropriate for mixed-species forests. Here we estimated 3-PG parameters for twelve major central European tree species using 1418 long-term permanent forest monitoring plots from managed forests, 297 from un-managed forest reserves and 784 Swiss National Forest Inventory plots. A literature review of tree physiological characteristics, as well as regression analyses and Bayesian inference, were used to calculate the 3-PG parameters.

The Swiss-wide calibration, based on monospecific plots, showed a robust performance in predicting forest stocks such as stem, foliage and root biomass. The plots used to inform the Bayesian calibration resulted in posterior ranges of the calibrated parameters that were, on average, 69% of the prior range. The bias of stem, foliage and root biomass predictions was generally less than 20%, and less than 10% for several species. The parameter sets also provided reliable predictions of biomass and mean tree sizes in mixed-species forests. Given that the information sources used to develop the parameters included a wide range of climatic, edaphic and management conditions and long time spans (from 1930 to present), these species parameters for 3-PG are likely to be appropriate for most central European forests and conditions.

Keywords Forest simulator · Data assimilation · Bayesian calibration · Forest inventory · Mixed-species forests · Permanent growth experiments

Introduction

Foresters, policy makers and scientists often use models to estimate forest biomass or wood production, carbon budgets, and the impacts of climate change, management, or

✉ David I. Forrester
david.forrester@wsl.ch

1 Swiss Federal Institute for Forest, Snow and Landscape Research WSL, Zuercherstrasse 111, 8903 Birmensdorf, Switzerland

2 Faculty of Forestry and Wood Sciences, Department of Forest Ecology, Czech University of Life Sciences Prague, Prague, Czech Republic

3 Department of Environmental Systems Science, Institute of Agricultural Sciences, ETH Zurich, 8092 Zurich, Switzerland

different species mixtures on growth. Many models have been developed that vary greatly in spatial and temporal resolutions, model complexity and the degree to which they rely on statistical relationships between variables versus the physiological processes of the system (Battaglia and Sands 1998; Fontes et al. 2010; Korzukhin et al. 1996; Pretzsch et al. 2015). Statistical models, or statistical model components, use equations and parameters derived from data sets representative of the conditions of interest (Korzukhin et al. 1996; Pretzsch et al. 2015; Vanclay and Skovsgaard 1997). However, such data sets are often not available for the range of conditions of interest to the model users, for example in areas where a species has not previously been present, or when new silvicultural treatments are of interest, or as new climatic conditions arise. In contrast, process-based models, or models with some process-based components, have been developed to overcome this limitation by simulating the

physiological processes that influence growth and how these processes are influenced by the environment.

Parameters used for process-based models are often derived from measurements of physiological processes, such as light absorption, transpiration, carbon partitioning and nutrient cycling (Minunno et al. 2019; Pretzsch et al. 2015). Intensive physiological measurements of many processes are often used to calibrate process-based models (e.g. Battaglia et al. 2004; Duursma and Medlyn 2012; Gonzalez-Benecke et al. 2016; Pietsch et al. 2005; Wei et al. 2014). However, measurements required to directly calculate all parameters are not often available. Therefore, many studies use trial and error to calibrate process-based models such that intensive physiological measurements and growth and yield data are used to calculate most parameters, while remaining parameters are tuned to maximize correlations between predictions and observations (e.g. Sands and Landsberg 2002). In other studies, the parameters are calculated using statistical fits of the given parameter as a function of stand characteristics that were calculated by the model (e.g. Gonzalez-Benecke et al. 2016).

A potential difficulty faced when measuring physiological processes is that measurements are not often possible for all species provenances within the region/s where the process-based models are to be applied and may therefore inadequately represent the physiology, morphology or phenology of the given species. Even when accurately measured parameter values are obtained, given that models are simplifications of reality, their parameters can play slightly different roles than their parameter name implies (van Oijen 2017). Therefore, the value of a parameter that produces the most realistic model behaviour may differ from the measured value (van Oijen 2017). To address this uncertainty, process-based model predictions can be improved when observations of outputs are used to constrain parameter values during model calibration (Hartig et al. 2012; Thomas et al. 2017; van Oijen 2017; van Oijen et al. 2005). While this means that the outputs will depend on the observed data in a similar way to statistical models (Minunno et al. 2019), it increases the reliability of the predictions for the region where the observed data were obtained. Several studies used inverse model-data assimilation methods such as Bayesian calibration to examine the uncertainty of parameters or model structures and to provide statistical distributions of parameter values (Fer et al. 2018; Gertner et al. 1999; Hartig et al. 2012; Minunno et al. 2019; Thomas et al. 2017; van Oijen 2017; van Oijen et al. 2013).

The forests of central Europe, such as in Switzerland, cover many environmental conditions and species compositions. Therefore, the objective of this study was to use Bayesian calibration to obtain parameters for the 3-PG model (Physiological Processes Predicting Growth; Forrester and Tang 2016; Landsberg and Waring 1997) for

twelve central European tree species. To accomplish this, a literature review of potential parameter values was combined with analyses of data from 2499 forest inventory plots in Switzerland. Data from monospecific plots were used for the Bayesian calibration and validation to obtain the 3-PG parameters, while an additional validation was done using 13 mixed-species plots.

Methods

The 3-PG model

3-PG is a stand-level model with a monthly time step. It was initially developed for evergreen, even-aged monospecific forests (Landsberg and Waring 1997) and was recently further developed for deciduous, uneven-aged and mixed-species forests (Forrester and Tang 2016), i.e. as a cohort-based model. 3-PG consists of five sub-models: light, biomass production, water balance, allocation and mortality. The light sub-model calculates light absorption using species-specific light extinction coefficients, leaf area indices and, in the case of multi-species or multi-cohort stands, the vertical positioning of each cohort based on species-specific mean height and crown length (Forrester et al. 2014). The biomass production sub-model calculates gross primary productivity based on a species-specific canopy quantum efficiency (α_C) that is reduced by limitations caused by temperature, frost, vapour pressure deficit, soil moisture, soil nutrient status, atmospheric CO_2 and stand age (Almeida et al. 2009; Landsberg and Waring 1997; Sands and Landsberg 2002). Net primary productivity is calculated as a constant fraction of gross primary productivity (Waring et al. 1998). In the water balance sub-model, transpiration and soil evaporation are calculated using the Penman–Monteith equation (Monteith 1965; Penman 1948). These are added to canopy interception to predict evapotranspiration. Soil water is calculated as the difference between evapotranspiration and rainfall, while draining off any water in excess of the maximum soil water holding capacity (Sands and Landsberg 2002). The biomass allocation sub-model distributes net primary productivity to roots, stems and foliage depending on soil nutrient status, vapour pressure deficit, soil moisture and tree size. The mortality sub-model calculates density-dependent mortality based on the −3/2 self-thinning law by Yoda et al. (1963) and density-independent mortality, e.g. caused by pests, diseases or drought (Gonzalez-Benecke et al. 2014; Sands 2004). The simulated biomass is converted into output variables such as mean tree diameter, height, basal area, wood volume and size distributions using allometric relationships. All sub-models have been validated by comparing predicted outputs from the given sub-model with measurements of the same process, such as transpiration, light absorption,

carbon partitioning and mortality (Gupta and Sharma 2019; Landsberg and Sands 2011). This piece-wise approach to validation reduces the likelihood of developing compensating errors among sub-models (Korzukhin et al. 1996; Sands 2004) that can be hidden by only validating a specific selection of the outputs, such as growth, stand density and mortality. 3-PG was run using the *r3PG* package (Trotsiuk et al. 2020) in R (R Core Team 2019). A description of all 3-PG parameters is provided in Table S1. When running *r3PG*, we used *settings = list(light_model = 2, transp_model = 2, phys_model = 2, height_model = 2, correct_bias = 1, calculate_d13c = 0)*. Therefore, the parameter sets developed from this study are most appropriate for these settings.

Forest inventory data

We used data from three permanent plot networks: long-term forest monitoring plots from managed forests and experiments from the Swiss Experimental Forest Management (EFM) network (Forrester et al. 2019), un-managed plots from the Swiss Forest Reserve Network (FRN) (Hobi et al.

2020) and the Swiss National Forest Inventory (NFI) (Fischer and Traub 2019; WSL 2020) (Fig. 1).

The EFM and FRN have been monitored following almost identical methodologies. They consist of long-term permanent plots, with the oldest plots monitored since 1888 and 1955, respectively. The EFM is used to examine silvicultural treatments across a range of species, climate and edaphic conditions. In contrast, the FRN acts as a reference for un-managed conditions. The average measurement intervals for the EFM data are 6.3 years (minimum of 1 and maximum of 29) and for the FRN plots are 12 years (minimum of 1 and maximum of 27). These intervals depend on the growth rates, stand age and research objectives. All individual trees with a diameter at a height of 1.3 m (d) $\geq$ 4 cm, for FRN plots, or $\geq$ 8 cm for EFM plots, are measured. For each tree, the d, status, and species are recorded. Tree height, crown diameter and crown length are measured for a subset of trees. For the EFM plots, age is calculated based on the planting or regeneration date, and measurements are taken at the same time as thinning to ensure an accurate recording of trees that are thinned and trees that die. Age is usually not available for the FRN plots, so we only used FRN data for
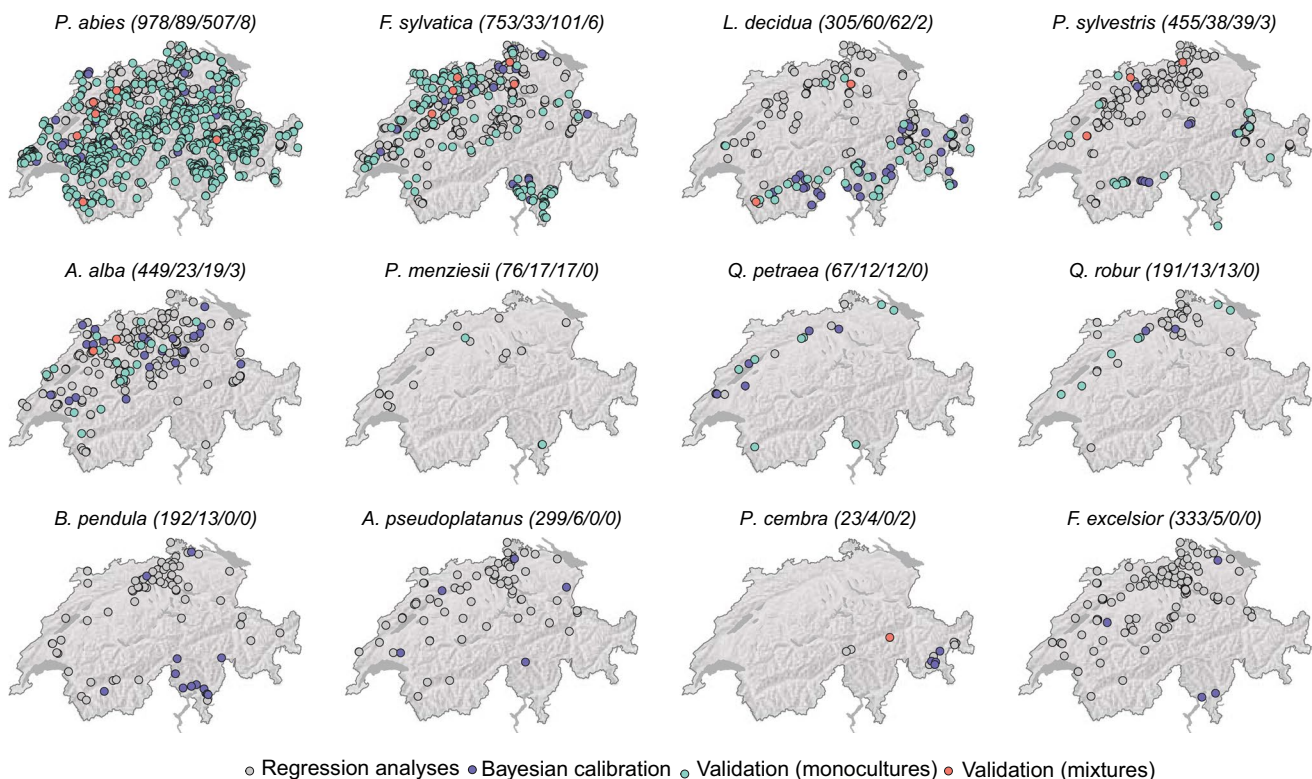

Fig. 1 Location of the monitoring plots used for the estimation of allometric or size-distribution parameters (e.g. based on regression analyses), as well as the Bayesian calibration and validation. Numbers in parentheses indicate the number of plots used for each category in the legend. Note that some EFM and FRN plots with different management strategies or site/topographic characteristics are located at the same location and are therefore overlapping on the maps

purposes where age information was not required. In this study, the time span between the first and the last measurement (time series length) for a given plot of the EFM and FRN ranged between 2 and 121 years (mean 26 years). For the Bayesian calibration, we only used data collected after the 1930s because the climatic data (required by 3-PG) were less reliable prior to 1930. All plots and data were used for parameter estimation using regression analyses.

The NFI plots are distributed on a regular grid of 1.4 km including about 6,500 permanent monitoring plots that have been measured at approximately 10-year intervals since 1983. They are circular nested plots where every tree with a $d \geq 12$ cm is recorded within an inner 200-m^2 circle (horizontal radius = 7.98 m), and every tree with a $d \geq 36$ cm is recorded within a 500-m^2 circle (horizontal radius = 12.62 m). For every individual tree, the d, crown length, status and species are recorded. Tree height and diameter at a height of 7 m are measured for a subset of trees. Age is estimated using a regression model that was fit to the data obtained either from counting tree rings or from counting layers of branch whorls (for conifers) directly on the plot (Fischer and Traub 2019). The trees lost due to thinning or mortality are derived from inventory data. In this study, the time span between the first and the last measurements (time series length) for a given NFI plot ranged between 5 and 34 years (mean 21 years).

The EFM/FRN complements the NFI network in terms of their variability and accuracy. That is, parameter uncertainty, and hence output uncertainty, can be reduced by increasing the variety of data used for calibration, increasing the accuracy of the measurements and increasing the lengths of the time series (van Oijen et al. 2005). The NFI plots increase the range of climatic and edaphic conditions because they have been distributed on a regular grid through Swiss forests and therefore increase the range of conditions already accounted for by the EFM/FRN plots. Thomas et al. (2017) found that calibrations using environmental gradients can constrain parameters associated with water and nutrient sensitivity to a similar degree as nutrient, drought and irrigation experiments. The EFM/FRN plots increase the data accuracy compared with the NFI plots, which have less accurate information about tree status (e.g. whether a tree died or was thinned) and tree age. Minunno et al. (2019) showed that more accurate calibration can be obtained with more accurate inventory data, such as long-term experimental plots (e.g. EFM and FRN) rather than plots with less accurate information about variables such as ages and tree status. The EFM plots also increase the lengths of the time series. For example, although our data set did not include any CO_2 fertilization experiments, which are useful for calibrating the 3-PG CO_2 parameters (Thomas et al. 2017), the EFM data (pre-1950s to 2019) cover periods with atmospheric $CO_2 < 320$ ppm to > 400 ppm. A summary of stand and site

characteristics for all plot networks combined is shown in Table 1.

Climate and soil data

Climate data were obtained by interpolation (100 m spatial resolution) using the DAYMET method (Thornton et al. 1997) by the Landscape Dynamics group (WSL, Switzerland) using data from MeteoSwiss stations (Swiss Federal Office of Meteorology and Climatology). Site-specific plant available soil water was retrieved from the European soil database derived data (Panagos et al. 2012). No site-specific information about soil fertility was available to estimate the 3-PG input variable that defines soil fertility (FR). Previous studies have used site indices, climate data and available soil water to calculate soil fertility (e.g. Forrester et al. 2017a). That is, by assuming the site index is mainly a function of soil fertility, available soil water and climate, then if only soil fertility is unknown, it can be calculated from the other variables. However, calculations of site index (based on age and height) were not considered reliable enough to use for this study because many plots lacked accurate age data, and therefore, we followed a simpler approach from several previous studies using 3-PG (Coops and Waring 2011; Mathys et al. 2014) where the FR for all sites and species was set to 0.5 for the Bayesian calibration and validation based on monospecific plots.

Plot selection

Subsets of EFM, FRN and NFI data were used for five main calculation steps: (1) 1418 EFM and 297 FRN plots were used for regression-based estimation of many allometric parameters, size-distribution parameters and parameters describing the fraction of mean single-tree foliage, stem or root biomass lost per dead tree (m_F, m_S, m_R), (2) Bayesian calibration based on a subset of 161 EFM and 152 NFI monospecific plots, (3) validation based on a different subset of 138 EFM and 632 NFI monospecific plots that were not used for calibration, (4) Bayesian calibration after combining all plots used for steps 2 and 3 (i.e. to obtain a final parameter set) and (5) validation based on 13 mixed-species EFM plots and the parameter sets develop in step 4. These data sets focused on twelve major European species shown in Table 1.

Step 1—estimation of parameters based on regression analyses

For the first step, parameters associated with tree allometry and size distributions were calculated using regression analyses based on 1418 EFM and 297 FRN plots (Fig. 1). The allometric parameters of 3-PG are used to calculate mean tree height, crown diameter, crown length and volume from

Table 1 Summaries of plot and site characteristics by species for all plots (EFM, FRN and NFI) used in this study. These species were selected because they were the twelve most abundant in our data set. Relative height is the mean height of the species divided by the mean height of all trees in the plot. Note that not all plots were used for any single purpose (Bayesian calibration, validation, parameter estimation using regression analyses)

Species	Number of plots	First/last measurement	Mean plot size (min/max) ha	Mean total basal area (min/max) m² ha⁻¹	Mean d (min/max)	Mean trees per ha (min/max)	Mean species proportion by basal area (min/max)	Mean relative height (min/max)	Elevation (m a.s.l.)	Precipitation (mm yr⁻¹)	Average temperature (°C)
Abies alba	605	1888/2019	0.5 (0.02/11)	42.4 (0.2/98.3)	27.3 (8.1/83.4)	815 (24/3835)	0.32 (<0.01/1)	0.94 (0.16/3.87)	805 (357/1741)	1360 (989/1872)	7.2 (4.9/8.8)
Acer pseudoplatanus	378	1921/2019	0.43 (0.01/11)	37 (0/97.3)	20.9 (8/64.4)	705 (7/3667)	0.17 (<0.01/1)	0.94 (0.16/1.84)	837 (336/1650)	1379 (866/1774)	7 (5.2/9.2)
Betula pendula	74	1888/2019	0.38 (0.03/3.06)	29.9 (1.6/71.5)	20.1 (8/41.9)	1132 (108/3256)	0.11 (<0.01/1)	1.09 (0.29/1.96)	588 (360/1000)	1629 (634/2179)	7.1 (2.5/9.8)
Fagus sylvatica	988	1888/2019	0.38 (0.01/11)	35.5 (0.1/91.9)	22.6 (8/76.2)	780 (10/3407)	0.4 (<0.01/1)	0.93 (0.11/1.74)	681 (336/1531)	1401 (930/2354)	7.6 (4/9.4)
Fraxinus excelsior	375	1888/2019	0.44 (0.01/11)	35 (1.1/76.5)	22.9 (8/74.4)	846 (50/2785)	0.11 (<0.01/1)	1.01 (0.29/2.23)	621 (336/1273)	1555 (956/2054)	9 (8.2/9.5)
Larix decidua	415	1889/2019	0.31 (0/11)	35.4 (0/97.3)	31.2 (8.1/85.9)	816 (6/3838)	0.49 (<0.01/1)	1.12 (0.31/3.06)	1035 (217/2130)	1373 (754/2226)	5.9 (0.5/12)
Picea abies	1605	1888/2019	0.31 (0.01/11)	41.2 (0/98.3)	28.4 (8/84.3)	894 (5/4990)	0.53 (<0.01/1)	1 (0.22/2.33)	943 (282/2065)	1534 (779/2772)	5.1 (0.7/11.4)
Pinus cembra	56	1905/2019	0.54 (0.05/3.33)	40.9 (1.3/77.2)	30.1 (9/69.9)	917 (50/4990)	0.19 (<0.01/0.38)	1 (0.65/1.21)	1774 (1475/2102)	1075 (1001/1201)	1.5 (0.8/2.2)
Pinus sylvestris	511	1888/2019	0.27 (0.01/2.5)	37.7 (0.9/86.6)	28.7 (8.3/65.8)	1060 (36/4814)	0.38 (<0.01/1)	1.15 (0.56/2.5)	677 (336/1998)	1185 (666/1892)	7.4 (1.5/11.3)
Pseudotsuga menziesii	79	1906/2018	0.23 (0.02/1.61)	34.3 (0.3/91.2)	27.3 (8.3/84.4)	796 (39/2500)	0.85 (<0.01/1)	1.05 (0.64/2.96)	549 (445/950)	1207 (1083/1811)	9 (8.8/9.8)
Quercus petraea	82	1914/2019	0.23 (0.03/2)	27.8 (5.9/68.2)	29 (8.4/71.5)	766 (88/2435)	0.64 (<0.01/1)	1.18 (0.48/2.7)	548 (420/1197)	1112 (914/2116)	8.6 (6.5/10.1)
Quercus robur	214	1914/2019	0.31 (0/1.32)	32.7 (5.7/99.1)	29.2 (8/82.9)	844 (197/2512)	0.46 (<0.01/1)	1.15 (0.67/1.88)	519 (337/875)	1054 (914/1124)	8.6 (8.1/9.1)

variables such as mean d, age, stand density and relative height. The selection criteria for these plots were that all variables required by the allometric equations were available (e.g. d, height, crown length, crown diameter, age, basal area). Since age was usually not available for FRN plots, these could only be used for regressions without age. An additional criterion for plots used to obtain parameters used to describe diameter distributions and stem mass distributions was that the given species was even-aged and hence had unimodal-shaped distributions. That is, the stand can be uneven-aged without a unimodal-shaped size distribution (e.g. where one species is older than another), but the trees from a given species must appear to be about the same age based on plot records and visual inspection of size distributions.

The height and live-crown length equations were fit as nonlinear equations using the *nls* function in R 3.5.1 (R Core Team 2019). The volume, crown diameter and Weibull parameter functions were fit as hierarchical mixed-effect models using the *lme* function of the *nlme* R package (Pinheiro et al. 2018). Initially all fixed effect variables were included before all non-significant ($P > 0.05$) variables were removed in order of decreasing P-value. Residual and normal quantile plots were assessed to ensure that residuals were centred at zero and approximately normally distributed. Plot was included as a random effect. For the mixed-effect models, a "pseudo" R^2 and conditional "pseudo" R^2 (R^2c) were calculated using the function *r.squaredGLMM* in the R package *MuMIn* (Bartoń 2016).

We used an alternative height and live-crown length equation to the earlier equation described in Forrester and Tang (2016). This alternative equation was a Michajlow (or Schumacher) function (Michajlow 1952) (Eq. 1):

$$y = 1.3 + a \times e^{-n_B/d} + n_C \times C \times d \qquad (1)$$

where y is height or live-crown length in metres, C is the competition variable of 3-PG indicating stand density, and a, n_B and n_C are fitted parameters used for 3-PG.

3-PG calculates d and stem mass distributions as Weibull distributions using shape, scale and location variables. Each of these variables is calculated as a function of mean tree or stand characteristics, and the parameters of these functions are 3-PG parameters. These can be calculated using data from monocultures or mixtures, but in mixed-species plots, the number of trees in each size class is divided by the species proportion (in terms of basal area) before fitting the equations (Tables S6–S11). The fractions of mean single-tree foliage, stem or root biomass lost per dead tree (m_F, m_S, m_R) (Table S1) were calculated from the slope of the relationship between the proportion of stand foliage, stem or root biomass of dead trees and the proportion of the number of trees lost due to mortality (Landsberg et al.

2005). Detailed descriptions of parameter estimation (based on regressions) or calculations using literature sources are provided in Forrester (2020).

Step 2—Bayesian calibration

Bayesian inference was used to derive parameter estimates and uncertainties for 18 parameters (Table 2). These 18 parameters were selected because they could not be calculated directly from our data, such as those in step 1, and sensitivity analyses have shown that 3-PG is sensitive to these parameters (Almeida et al. 2004; Esprey et al. 2004; Forrester and Tang 2016; Law et al. 2000; Mathys et al. 2014; Meyer et al. 2017; Navarro-Cerrillo et al. 2016; Pérez-Cruzado et al. 2011; Potithep and Yasuoka 2011; Xenakis et al. 2008). This step was based on 161 EFM and 152 NFI plots. The selection criteria were: (1) that the plots were monospecific and even-aged, (2) with at least two consecutive measurements, (3) no ingrowth, such that any pairs of consecutive measurements with ingrowth were excluded, (4) no obvious measurement errors, and (5) stand age was known. No FRN plots were used for calibration or validation because they are generally mixed-species and uneven-aged plots without age information. Monocultures were defined as plots where more than 80% of the basal area was composed of the object species. If the object species occupied > 80% but < 100% of plot basal area, its biomass stocks were adjusted by dividing by its proportional contribution of basal area to the plot. Mixed-species plots could not be used for Bayesian calibration because each species within a mixture would need to be calibrated simultaneously. Therefore, since most species occurred in different types of mixtures, most species would have needed to be calibrated simultaneously, which was beyond the scope of this study. An additional criterion for the NFI plots were that there was no thinning because thinning, as opposed to mortality, is difficult to measure accurately in the NFI plots. Thinned plots were not excluded from the EFM network.

This Bayesian inference approach requires a prior range between which the parameter for the given species can occur. We assumed uniform (i.e. non-informative) prior distributions for each of the 18 model parameters. If many published values were available for a given parameter and species, the prior range was set as the minimum and maximum values (Table S12) plus or minus 15% (Table 2). For the less commonly measured parameters and species, we set the prior ranges to the mean value found in the literature for that species (Table S12) or other species considered similar in terms of the given parameter, plus or minus 20% (Table 2).

The first calibrations indicated that the prior ranges of the self-thinning parameters (*wSx1000* and thinPower in Tables 2 and S1) were too narrow, despite many published studies informing the prior ranges. In contrast, the upper

Table 2 Prior ranges of each parameter included in the Bayesian calibration. These ranges were made by using information from the literature review (Table S12)

Parameter	Abies alba	Acer pseudo-platanus	Betula pen-dula	Fagus syl-vatica	Fraxinus excelsior	Larix decidua	Picea abies	Pinus cem-bra	Pinus sylves-tris	Pseudotsuga menziesii	Quercus petraea	Quercus robur
pFS2	0.0300–1.7000	0.0300–1.7000	0.0300–1.7000	0.0300–1.7000	0.0300–1.7000	0.0300–1.7000	0.0300–1.7000	0.0300–1.7000	0.0300–1.7000	0.0300–1.7000	0.0300–1.7000	0.0300–1.7000
pFS20	0.0100–0.8000	0.0100–0.8000	0.0100–0.8000	0.0100–0.8000	0.0100–0.8000	0.0100–0.8000	0.0100–0.8000	0.0100–0.8000	0.0100–0.8000	0.0100–0.8000	0.0100–0.8000	0.0100–0.8000
pRx	0.2000–0.8000	0.2000–0.8000	0.2000–0.8000	0.2000–0.8000	0.2000–0.8000	0.2000–0.8000	0.2000–0.8000	0.2000–0.8000	0.2000–0.8000	0.2000–0.8000	0.2000–0.8000	0.2000–0.8000
pRn	0.0500–0.3000	0.0500–0.3000	0.0500–0.3000	0.0500–0.3000	0.0500–0.3000	0.0500–0.3000	0.0500–0.3000	0.0500–0.3000	0.0500–0.3000	0.0500–0.3000	0.0500–0.3000	0.0500–0.3000
gammaF1	0.0000–0.0122	*	*	*	*	*	0.0000–0.0138	0.0000–0.0221	0.0000–0.0337	0.0000–0.0164	*	*
gammaR	0.0000–0.2000	0.0000–0.2000	0.0000–0.2000	0.0000–0.2000	0.0000–0.2000	0.0000–0.2000	0.0000–0.2000	0.0000–0.2000	0.0000–0.2000	0.0000–0.2000	0.0000–0.2000	0.0000–0.2000
Tmin	−5–5	−2–6	−2–6	−2–6	−2–6	−2–6	−5–2.5	−5–2.5	−5–5	−5–2.5	−2–6	−2–6
Topt	15–25	15–25	15–25	15–25	15–25	15–25	15–25	15–25	15–25	15–25	15–25	15–25
Tmax	30–45	30–45	30–45	30–45	30–45	30–45	30–45	30–45	30–45	30–45	30–45	30–45
fCalpha700	1.0000–1.4500	1.0000–1.4500	1.0000–1.4500	1.0000–1.4500	1.0000–1.4500	1.0000–1.4500	1.0000–1.4500	1.0000–1.4500	1.0000–1.4500	1.0000–1.4500	1.0000–1.4500	1.0000–1.4500
fCg700	0.4500–1.0000	0.4500–1.0000	0.4500–1.0000	0.4500–1.0000	0.4500–1.0000	0.4500–1.0000	0.4500–1.0000	0.4500–1.0000	0.4500–1.0000	0.4500–1.0000	0.4500–1.0000	0.4500–1.0000
wSx1000	219.05–328.58	247.42–371.13	116.06–174.10	291.31–436.97	299.47–449.21	178.10–267.15	257.50–386.25	120.17–180.25	136.71–205.07	201.74–302.62	151.46–227.19	151.46–227.19
thinPower	1.3648–2.0472	1.4284–2.1426	1.8648–2.4000	1.4452–2.1679	1.5512–2.3268	1.5488–2.3232	1.3243–1.9865	1.2000–1.8000	1.3372–2.0058	1.2720–1.9080	1.2887–1.9331	1.2887–1.9331
k	0.3000–0.6500	0.3000–0.6500	0.3000–0.6500	0.3000–0.6500	0.3000–0.6500	0.3000–0.6500	0.3000–0.6500	0.3000–0.6500	0.3000–0.6500	0.3000–0.6500	0.3000–0.6500	0.3000–0.6500
MaxIntcptn	0.2880–0.4000	0.1810–0.2715	0.1412–0.2118	0.2188–0.3282	0.2093–0.3139	0.1400–0.2100	0.2201–0.3302	0.2738–0.4000	0.2738–0.4000	0.2670–0.4000	0.1352–0.2028	0.1384–0.2076
alphaCx	0.0250–0.0700	0.0250–0.0700	0.0250–0.0700	0.0250–0.0700	0.0250–0.0700	0.0250–0.0700	0.0250–0.0700	0.0250–0.0700	0.0250–0.0700	0.0250–0.0700	0.0250–0.0700	0.0250–0.0700
MaxCond	0.0100–0.0350	0.0160–0.0240	0.0160–0.0240	0.0171–0.0256	0.0100–0.0350	0.0100–0.0350	0.0244–0.0350	0.0100–0.0350	0.0123–0.0184	0.0180–0.0269	0.0188–0.0282	0.0160–0.0240
CoeffCond	0.0760–0.1000	0.0368–0.0552	0.0421–0.0632	0.0418–0.0627	0.0426–0.0639	0.0752–0.1000	0.0763–0.1000	0.0200–0.1000	0.0607–0.0911	0.0419–0.0629	0.0388–0.0582	0.0376–0.0564

*Not applicable for deciduous species

limit of the prior ranges for the T_{min} parameter was too high for *P. abies*, *P. cembra* and *P. menziesii* and was reduced to 2.5, as informed by the literature (Table S12). Note that the T_{min} parameter of 3-PG represents a mean monthly minimum temperature (i.e. monthly-T_{min}) where the species can no longer grow. However, this value will probably be lower than the actual daily T_{min} (daily-T_{min}) that determines whether growth is possible for the given species, because even when the monthly-T_{min} is lower than the daily-T_{min}, there are likely to be several days during that month where the minimum temperature is higher than the daily-T_{min}, and hence, some growth will still occur for that month. The reduction of T_{min} to 2.5 was required because T_{min} is multiplied by the canopy quantum efficiency parameter, α_{Cx}, to calculate gross primary production. The overestimation of T_{min} restricted growth to warmer months, and the resulting reduction in annual growth was compensated for by an overestimation of α_{Cx}.

The likelihood function was constructed to be robust against outliers by modelling the residual error as a Student's t distribution with sampled degrees of freedom (see Code S1; Lange et al. 1989), following Augustynczik et al. (2017). For each calibration, we parametrized the degrees of freedom of the output variable using the constant of the probability of having outliers in the dataset and estimated the parameter using a uniform prior distribution from 0 to 1. The variance of each observation was estimated using the uniform prior distribution specific for each variable: stem biomass (0–50), foliage biomass (0–5) and root biomass (0–15). The joint posterior distribution for the model parameters was estimated using a Differential Evolution Markov Chain Monte-Carlo algorithm (DEzs MCMC, ter Braak and Vrugt 2008) implemented in the *BayesianTools R* package (Hartig et al. 2019). For each species, three independent DEzs MCMC runs were made, each with three internal chains. Convergence was tested by visual inspection of the trace plots and using the Gelman–Rubin diagnostic (Gelman and Rubin 1992). Convergence was accepted when the multivariate potential scale reduction factor was ≤ 1.1. Three independent DEzs MCMC chains with 2×10^6 iterations were required to achieve convergence. All analyses and calculations were performed in the *R* language for statistical computing (R Core Team 2019).

For calibration, we used three variables that describe stand stocks: stem biomass (SB), foliage biomass (FB) and root biomass (RB). Stem, root and foliage biomass were calculated for each measured tree using equations developed for European forests (Forrester et al. 2017b) and summed up to the stand level in Mg dry matter ha^{-1}. The fractions of mean single-tree foliage, stem or root biomass lost per thinned tree (*F, S, R*) were calculated for each plot and growth period as the ratio of the proportion of stand foliage, stem or root biomass of thinned trees and the proportion of the number

of trees lost due to thinning. The first observations on each monitoring plot were used to initialize the 3-PG model runs (see below), while the subsequent observations were used to calculate likelihood for DEzs MCMC runs (Tables 3 and 4).

Step 3—3-PG model evaluation and validation for monocultures

The validation of monospecific plots was based on the same criteria as the plots used for Bayesian calibration and included 138 EFM and 632 NFI plots that had not been used for the calibration. For species where the total number of plots was above 30, we randomly split the full set of monitoring data into two equally sized groups, resulting in a calibration and a validation set. For the two *Quercus* species, we used 70% of the total number of plots for calibration and 30% for validation. For the rest of the species, we used all available monitoring plots for calibration.

The skill of the 3-PG model to generate model predictions was assessed using posterior predictive distributions obtained by running the model with 1,000 random samples from the parameters' posterior distribution. The model performance was evaluated using the percentage bias (pBias; Eq. 2), root mean squared error (RMSE; Eq. 3) and normalized root mean square error (NRMSE; Eq. 4). The statistics were calculated at the plot level and then averaged for each of the 1,000 parameter samples. The validation only used the most recent set of observations at each plot to maximize the time between initialization and validation, which ranged from 4 to 87 years.

The pBias, RMSE and NRMSE were calculated as

$$pBias = 100 \frac{\tilde{P} - \tilde{O}}{\tilde{O}} \tag{2}$$

$$RMSE = \sqrt{\frac{\sum_{i=1}^{n}(P_i - O_i)^2}{n}} \tag{3}$$

$$NRMSE = \frac{RMSE}{O_{max} - O_{min}} \tag{4}$$

where O_i are the observed values, P_i are the predicted values from 3-PG, $\tilde{O}$ and $\tilde{P}$ are the means and O_{max} and O_{min} are the maximum and minimum of the observed values.

Step 4—3-PG model calibration using all plots

The parameter estimates obtained in Step 2 were based on only about half of the plots, with the other half used for validation (Step 3). Therefore, a final set of parameters were

Table 3 Posterior ranges of each parameter included in the Bayesian calibration that was based only on the calibration plots

Parameter	Abies alba	Acer pseudoplatanus	Betula pendula	Fagus sylvatica	Fraxinus excelsior	Larix decidua	Picea abies	Pinus cembra	Pinus sylvestris	Pseudotsuga menziesii	Quercus petraea	Quercus robur
pFS2	0.5951 (0.1306–1.5827)	0.1269 (0.0327–1.3982)	1.2002 (0.2587–1.6793)	0.0380 (0.0303–0.0724)	0.9288 (0.1127–1.6558)	1.3231 (0.5670–1.6856)	0.6665 (0.4094–1.2084)	1.1724 (0.2740–1.6758)	0.0837 (0.0444–0.2196)	0.1889 (0.1401–0.2392)	0.6640 (0.2046–1.5498)	0.0662 (0.0367–0.1335)
pFS20	0.1165 (0.0458–0.2555)	0.0230 (0.0138–0.0406)	0.0266 (0.0172–0.0417)	0.0118 (0.0107–0.0134)	0.0445 (0.0205–0.1196)	0.0139 (0.0110–0.0172)	0.0904 (0.0716–0.1122)	0.2141 (0.0416–0.7426)	0.0470 (0.0303–0.0801)	0.1803 (0.1345–0.2244)	0.0348 (0.0295–0.0413)	0.0290 (0.0254–0.0333)
pRx	0.3370 (0.2083–0.7680)	0.4547 (0.2267–0.7747)	0.3710 (0.2094–0.7717)	0.3141 (0.2035–0.7546)	0.4760 (0.2536–0.7837)	0.4831 (0.2162–0.7838)	0.5940 (0.3270–0.7898)	0.5858 (0.2702–0.7920)	0.5283 (0.2957–0.7838)	0.2324 (0.2012–0.4129)	0.2812 (0.2066–0.6979)	0.3310 (0.2043–0.7502)
pRn	0.1081 (0.0540–0.2171)	0.1843 (0.0644–0.2921)	0.1164 (0.0556–0.2360)	0.0758 (0.0517–0.1188)	0.1441 (0.0592–0.2848)	0.0823 (0.0523–0.1315)	0.1030 (0.0551–0.1589)	0.2086 (0.0714–0.2950)	0.1880 (0.0772–0.2935)	0.1005 (0.0597–0.1308)	0.1512 (0.0649–0.2411)	0.0812 (0.0522–0.1235)
gammaF1	0.0039 (0.0006–0.0098)	*	*	*	*	*	0.0006 (0.0002–0.0011)	0.0024 (0.0001–0.0121)	0.0005 (0.0000–0.0014)	0.0124 (0.0085–0.0161)	*	*
gammaR	0.0001 (0.0000–0.0005)	0.0035 (0.0001–0.0180)	0.0001 (0.0000–0.0008)	0.0003 (0.0000–0.0011)	0.0006 (0.0000–0.0027)	0.0000 (0.0000–0.0002)	0.0002 (0.0000–0.0006)	0.0010 (0.0001–0.0026)	0.0024 (0.0008–0.0045)	0.0001 (0.0000–0.0007)	0.0010 (0.0001–0.0033)	0.0004 (0.0000–0.0014)
Tmin	1.2290 (−4.5182–4.8442)	0.7773 (−1.8610–5.4495)	0.0008 (−1.9282–4.4247)	5.6288 (4.0093–5.9837)	2.6581 (−1.7123–5.8528)	1.5773 (−1.2252–3.6939)	2.4200 (2.0568–2.4968)	1.0418 (−3.7690–2.4649)	1.1982 (−4.5331–4.8010)	1.6530 (−2.6337–2.4636)	2.8184 (−1.7343–5.8802)	2.9892 (−1.7105–5.8714)
Topt	21.8250 (15.5402–24.8690)	18.7148 (15.2134–24.3433)	18.7897 (15.1688–24.4297)	24.2466 (21.5073–24.9695)	22.4016 (15.5039–24.8667)	23.1970 (18.6806–24.9018)	24.8562 (24.2714–24.9947)	22.9700 (17.1123–24.9140)	22.2437 (15.7531–24.8967)	23.4876 (19.5345–24.9254)	20.6685 (15.5064–24.7498)	21.0282 (15.2827–24.8773)
Tmax	37.1982 (30.3344–44.5987)	38.2181 (30.5026–44.5881)	38.0739 (30.3709–44.7327)	33.6050 (30.1224–43.7907)	36.7143 (30.2979–44.5829)	36.1615 (30.2629–44.5365)	30.3944 (30.0134–32.3599)	35.5482 (30.2234–44.3074)	37.1471 (30.4705–44.5630)	36.1759 (30.2486–44.3072)	37.0831 (30.3599–44.5509)	36.7969 (30.3158–44.5847)
fCalpha700	1.1966 (1.0100–1.4379)	1.2372 (1.0130–1.4412)	1.2202 (1.0098–1.4341)	1.1634 (1.0118–1.4171)	1.2093 (1.0101–1.4379)	1.0631 (1.0020–1.3072)	1.0129 (1.0006–1.0658)	1.1960 (1.0098–1.4360)	1.0463 (1.0019–1.2810)	1.1766 (1.0071–1.4301)	1.1097 (1.0039–1.4091)	1.2933 (1.0286–1.4400)
fCg700	0.7069 (0.4608–0.9805)	0.7560 (0.4714–0.9888)	0.7469 (0.4644–0.9854)	0.8002 (0.4897–0.9905)	0.7149 (0.4638–0.9849)	0.7450 (0.4689–0.9869)	0.9094 (0.6599–0.9955)	0.7298 (0.4632–0.9855)	0.8077 (0.4920–0.9922)	0.6881 (0.4667–0.9796)	0.8449 (0.5295–0.9923)	0.6830 (0.4589–0.9809)
wSx1000	313.4620 (262.0103–328.0516)	309.4698 (250.7273–368.4414)	146.9729 (118.2070–172.7246)	327.0699 (293.4961–427.3635)	373.0627 (302.0151–445.0584)	225.7253 (180.7169–264.8341)	378.3186 (349.3645–385.9333)	177.3306 (138.9058–180.1897)	199.7051 (179.9574–204.8344)	213.3776 (202.1628–252.7485)	157.1333 (151.6941–180.9359)	154.4688 (151.5871–163.2787)
thinPower	1.9777 (1.7287–2.0442)	1.7795 (1.4447–2.1205)	2.1376 (1.8801–2.3837)	1.6966 (1.4556–2.1266)	1.9449 (1.5708–2.3085)	1.9527 (1.5818–2.3054)	1.7732 (1.6064–1.9640)	1.7806 (1.4426–1.7993)	1.4088 (1.3394–1.8389)	1.5887 (1.3143–1.8149)	1.5511 (1.4277–1.8579)	1.3107 (1.2902–1.3465)

Table 3 (continued)

Parameter	Abies alba	Acer pseudoplatanus	Betula pendula	Fagus sylvatica	Fraxinus excelsior	Larix decidua	Picea abies	Pinus cembra	Pinus sylvestris	Pseudotsuga menziesii	Quercus petraea	Quercus robur
k	0.5257 (0.3201–0.6426)	0.4211 (0.3045–0.6319)	0.5884 (0.3671–0.6475)	0.6107 (0.4611–0.6482)	0.4861 (0.3082–0.6390)	0.3093 (0.3004–0.3482)	0.4133 (0.3038–0.6363)	0.3890 (0.3032–0.6305)	0.4505 (0.3048–0.6393)	0.6009 (0.4536–0.6481)	0.6037 (0.4426–0.6476)	0.6064 (0.4291–0.6483)
MaxIntcptn	0.3385 (0.2904–0.3966)	0.2336 (0.1847–0.2697)	0.1784 (0.1429–0.2105)	0.2484 (0.2197–0.3179)	0.2615 (0.2117–0.3108)	0.1735 (0.1416–0.2083)	0.2295 (0.2206–0.2648)	0.3342 (0.2776–0.3969)	0.3684 (0.2831–0.3988)	0.3491 (0.2734–0.3972)	0.1721 (0.1376–0.2014)	0.1715 (0.1400–0.2058)
alphaCx	0.0283 (0.0251–0.0381)	0.0400 (0.0286–0.0607)	0.0298 (0.0253–0.0376)	0.0436 (0.0360–0.0526)	0.0265 (0.0251–0.0317)	0.0610 (0.0498–0.0694)	0.0401 (0.0342–0.0481)	0.0285 (0.0251–0.0443)	0.0258 (0.0250–0.0293)	0.0631 (0.0522–0.0696)	0.0408 (0.0311–0.0528)	0.0410 (0.0319–0.0522)
MaxCond	0.0144 (0.0102–0.0282)	0.0220 (0.0174–0.0239)	0.0210 (0.0163–0.0238)	0.0177 (0.0171–0.0200)	0.0235 (0.0138–0.0328)	0.0142 (0.0102–0.0238)	0.0247 (0.0245–0.0259)	0.0206 (0.0104–0.0343)	0.0176 (0.0144–0.0184)	0.0232 (0.0198–0.0266)	0.0253 (0.0194–0.0280)	0.0193 (0.0161–0.0238)
CoeffCond	0.0908 (0.0773–0.0997)	0.0456 (0.0372–0.0546)	0.0522 (0.0426–0.0627)	0.0569 (0.0438–0.0624)	0.0573 (0.0438–0.0635)	0.0836 (0.0756–0.0987)	0.0860 (0.0769–0.0986)	0.0800 (0.0284–0.0991)	0.0814 (0.0626–0.0907)	0.0514 (0.0424–0.0622)	0.0477 (0.0392–0.0578)	0.0462 (0.0379–0.0558)

*Not applicable for deciduous species

obtained by repeating Step 2 but after combining the calibration plots and validation plots.

Step 5—3-PG model evaluation and validation for mixtures

To test that the parameter sets also provided reliable predictions for mixed-species forests, 13 mixed-species plots were simulated by inputting information from the first inventory. The selection criteria for these plots were the same as the calibration plots, except that they needed to be mixed. Since site-specific soil fertility data were not available, the FR was adjusted to a value that gave satisfactory model performance. The parameters used were obtained in Step 4 and were based on all calibration and validation plots. pBias and RMSE were calculated for each species within the 13 mixed-species plots. Only the most recent set of observations for each plot were used to maximize the time between initialization and validation, which ranged from 16 to 47 years. The model performance was calculated using the pBias (Eq. 2) and the relationships between predictions and observations.

Results

Estimation of parameters based on regression analyses

By using the EFM and FRN data sets, large sample sizes were available for most regressions, and these samples generally included broad ranges in tree sizes and stand, or site conditions (Tables 1 and S2-S11). The statistical information for each regression is provided in Tables S2 to S11.

The mean tree height and live-crown length were often influenced by stand density, as well as d (Tables S2 and S3). Individual tree crown diameter was often influenced by stand density and relative height, in addition to d (Table S5). Mean tree volume was a function of d and height for all species (Table S4).

The scale, shape and location parameters that describe d and stem mass distributions varied between species in terms of which variables were significant (d, relative height, age and stand density). For several species with lower samples sizes (*A. pseudoplatanus, B. pendula, F. excelsior*), none of the explanatory variables were significant for at least one of the scale, shape and location parameters, and in those cases, the mean scale, shape or location parameter for the given species was used (Tables S6-S11).

Bayesian calibration

By using the Bayesian calibration, we were able to reduce the parametric uncertainty of 3-PG. The width of the posterior

Table 4 Parameters and their sources: *calculated from published studies (for sources, see Table S12), #calculated from EFM and FRN data (regression analyses), #posterior parameter estimates from Bayesian inference (using all calibration and validation plots; Step 4) and their quantiles (median and 2.5%–97.5% quantiles). For a description of the 3-PG parameters, see Table S1

Parameter	Abies alba	Acer pseudo-platanus	Betula	Fagus sylvatica	Fraxinus excelsior	Larix decidua	Picea abies	Pinus cembra	Pinus sylvestris	Pseudotsuga menziesii	Quercus petraea	Quercus robur
pFS2#	0.3745 (0.1044–1.3914)	0.1269 (0.0327–1.3982)	1.2002 (0.2587–1.6793)	0.0404 (0.0305–0.0737)	0.9288 (0.1127–1.6558)	0.8669 (0.3921–1.5892)	0.8297 (0.6455–1.0781)	1.1724 (0.2740–1.6758)	0.1673 (0.0716–0.6317)	0.1936 (0.1592–0.2223)	0.4330 (0.1531–1.3311)	0.0464 (0.0319–0.0759)
pFS20#	0.1084 (0.0505–0.2005)	0.0230 (0.0138–0.0406)	0.0266 (0.0172–0.0417)	0.0102 (0.0100–0.0110)	0.0445 (0.0205–0.1196)	0.0171 (0.0146–0.0196)	0.1480 (0.1346–0.1629)	0.2141 (0.0416–0.7426)	0.0457 (0.0329–0.0669)	0.1900 (0.1566–0.2171)	0.0350 (0.0296–0.0436)	0.0277 (0.0257–0.0299)
aWS*	0.082	0.1	0.11	0.183	0.074	0.187	0.133	0.128	0.126	0.082	0.094	0.056
nWS*	2.459	2.419	2.377	2.39	2.618	2.251	2.305	2.305	2.268	2.523	2.507	2.744
pRx#	0.3714 (0.2061–0.7649)	0.4547 (0.2267–0.7747)	0.3710 (0.2094–0.7717)	0.3600 (0.2069–0.7476)	0.4760 (0.2536–0.7837)	0.5170 (0.2282–0.7827)	0.7151 (0.5052–0.7972)	0.5858 (0.2702–0.7920)	0.3303 (0.2363–0.6612)	0.2261 (0.2008–0.3941)	0.2829 (0.2087–0.7025)	0.2773 (0.2020–0.7032)
pRn#	0.0946 (0.0538–0.1774)	0.1843 (0.0644–0.2921)	0.1164 (0.0556–0.2360)	0.0737 (0.0513–0.1020)	0.1441 (0.0592–0.2848)	0.0797 (0.0522–0.1197)	0.0824 (0.0522–0.1136)	0.2086 (0.0714–0.2950)	0.1619 (0.0634–0.2819)	0.1009 (0.0664–0.1217)	0.1541 (0.0647–0.2388)	0.0823 (0.0523–0.1213)
gammaF1#	0.0041 (0.0010–0.0093)	0	0	0	0	0	0.0008 (0.0007–0.0010)	0.0024 (0.0001–0.0121)	0.0004 (0.0000–0.0010)	0.0139 (0.0111–0.0162)	0	0
gammaF0*	0.001	0	0	0	0	0	0.001	0.001	0.001	0.001	0	0
tgammaF*	60	0	0	0	0	0	60	60	60	60	0	0
gammaR#	0.0000 (0.0000–0.0002)	0.0035 (0.0001–0.0180)	0.0001 (0.0000–0.0008)	0.0000 (0.0000–0.0002)	0.0006 (0.0000–0.0027)	0.0000 (0.0000–0.0001)	0.0000 (0.0000–0.0001)	0.0010 (0.0001–0.0026)	0.0009 (0.0002–0.0016)	0.0001 (0.0000–0.0006)	0.0010 (0.0001–0.0026)	0.0003 (0.0000–0.0012)
leafgrow†	0	5	5	5	5	5	0	0	0	0	5	5
leaffall†	0	11	11	11	11	11	0	0	0	0	11	11
Tmin#	2.3251 (−4.2206–4.8540)	0.7773 (−1.8610–5.4495)	0.0008 (−1.9282–4.4247)	5.6101 (−4.3298–5.9851)	2.6581 (−1.7123–5.8528)	−0.9212 (−1.9452–1.3757)	2.4727 (2.3503–2.4994)	1.0418 (−3.7690–2.4649)	0.1138 (−4.6644–4.5918)	2.0218 (0.1997–2.4817)	4.3827 (−1.1530–5.9617)	3.3836 (−1.6666–5.9109)
Topt#	22.1780 (15.9742–24.9048)	18.7148 (15.2134–24.3433)	18.7897 (15.1688–24.4297)	24.3224 (21.8819–24.9738)	22.4016 (15.5039–24.8667)	23.5986 (19.5727–24.9473)	24.9494 (24.7295–24.9983)	22.9700 (17.1123–24.9140)	22.2742 (16.1026–24.8644)	23.8252 (21.5450–24.9428)	22.5405 (16.8139–24.8897)	21.9658 (15.2649–24.8783)
Tmax#	36.8918 (30.3106–44.6260)	38.2181 (30.5026–44.5881)	38.0739 (30.3709–44.7327)	33.7392 (30.1384–43.8745)	36.7143 (30.2979–44.5829)	35.7847 (30.2095–44.4614)	30.1378 (30.0036–30.8131)	35.5482 (30.2234–44.3074)	37.4242 (30.3689–44.5029)	35.0977 (30.2299–43.9470)	35.9017 (30.2671–44.5486)	36.4944 (30.2272–44.6375)
kF†	1	1	1	1	1	1	1	1	1	1	1	1
fCalpha700#	1.1877 (1.0065–1.4349)	1.2372 (1.0130–1.4412)	1.2202 (1.0098–1.4341)	1.0109 (1.0005–1.0556)	1.2093 (1.0101–1.4379)	1.1891 (1.0193–1.4149)	1.0040 (1.0002–1.0217)	1.1960 (1.0098–1.4360)	1.0246 (1.0007–1.1326)	1.1786 (1.0101–1.4283)	1.0739 (1.0027–1.3614)	1.3481 (1.0963–1.4462)
fCg700#	0.7116 (0.4595–0.9855)	0.7560 (0.4714–0.9888)	0.7469 (0.4644–0.9854)	0.9319 (0.7256–0.9975)	0.7149 (0.4638–0.9849)	0.7697 (0.4739–0.9900)	0.9584 (0.8084–0.9983)	0.7298 (0.4632–0.9855)	0.8914 (0.5946–0.9958)	0.6487 (0.4650–0.9669)	0.8753 (0.5852–0.9944)	0.6467 (0.4579–0.9724)
m0†	0	0	0	0	0	0	0	0	0	0	0	0
fN0†	0.6	0.6	0.6	0.6	0.6	0.6	0.6	0.6	0.6	0.6	0.6	0.6
fNn†	1	1	1	1	1	1	1	1	1	1	1	1

Full caption: Table 4 Parameters and their sources: *calculated from published studies (for sources, see Table S12), #calculated from EFM and FRN data (regression analyses), #posterior parameter estimates from Bayesian inference (using all calibration and validation plots; Step 4) and their quantiles (median and 2.5%–97.5% quantiles), ‡calculated from EFM and FRN data (regression analyses), †default (Forrester and Tang 2016; Sands and Landsberg 2002). For a description of the 3-PG parameters, see Table S1

Table 4 (continued)

Parameter	Abies alba	Acer pseudoplatanus	Betula	Fagus sylvatica	Fraxinus excelsior	Larix decidua	Picea abies	Pinus cembra	Pinus sylvestris	Pseudotsuga menziesii	Quercus petraea	Quercus robur
MaxAge*	550	493	149	400	300	650	400	900	600	600	725	922
nAge†	4	4	4	4	4	4	4	4	4	4	4	4
rAge†	0.95	0.95	0.95	0.95	0.95	0.95	0.95	0.95	0.95	0.95	0.95	0.95
gammaN1†	0	0	0	0	0	0	0	0	0	0	0	0
gammaN0†	0	0	0	0	0	0	0	0	0	0	0	0
tgammaN†	0	0	0	0	0	0	0	0	0	0	0	0
ngammaN†	1	1	1	1	1	1	1	1	1	1	1	1
wSx1000#	316.1296 (272.3703–328.0729)	309.4698 (250.7273–368.4414)	146.9729 (118.2070–172.7246)	350.1602 (315.4102–404.5037)	373.0627 (302.0151–445.0584)	212.0935 (179.1228–263.8702)	376.0843 (361.5013–385.7610)	177.3306 (138.9058–180.1897)	202.3125 (192.6945–204.9971)	204.1674 (201.8222–214.8934)	158.1916 (151.6991–183.7460)	155.2194 (151.6247–164.3961)
thinPower#	1.9833 (1.7641–2.0446)	1.7795 (1.4447–2.1205)	2.1376 (1.8801–2.3837)	2.0169 (1.8147–2.1583)	1.9449 (1.5708–2.3085)	2.1788 (1.8584–2.3160)	1.8740 (1.7626–1.9740)	1.7806 (1.4426–1.7993)	1.6025 (1.4756–1.7722)	1.6539 (1.5280–1.7684)	1.5916 (1.4122–1.9026)	1.3107 (1.2899–1.3468)
mF‡	0.492	0.451	0.412	0.487	0.465	0.409	0.488	0.606	0.558	0.464	0.446	0.419
mR‡	0.446	0.412	0.373	0.416	0.429	0.312	0.436	0.573	0.48	0.391	0.409	0.379
mS‡	0.444	0.401	0.363	0.418	0.419	0.321	0.437	0.571	0.481	0.409	0.376	0.333
SLA0*	12.32	23.94	13.05	24.72	30.3	13.83	8.71	4.6	4.29	6.56	18.49	18.49
SLA1*	5.85	14.93	13.05	19.4	12.6	11.72	3.85	4.6	4.29	5	14.62	14.62
tSLA*	18.1	47	1	35	13.6	14.5	25.1	1	1	44.7	7.35	7.35
k#	0.6024 (0.4644–0.6480)	0.4211 (0.3045–0.6319)	0.5884 (0.3671–0.6475)	0.6260 (0.5259–0.6490)	0.4861 (0.3082–0.6390)	0.6279 (0.5165–0.6492)	0.6378 (0.5934–0.6496)	0.3890 (0.3032–0.6305)	0.3247 (0.3012–0.4558)	0.6153 (0.5088–0.6486)	0.5952 (0.4359–0.6479)	0.6171 (0.4818–0.6491)
fullCanAge†	3	3	3	3	3	3	3	3	3	3	3	3
MaxIntcptn#	0.3381 (0.2907–0.3971)	0.2336 (0.1847–0.2697)	0.1784 (0.1429–0.2105)	0.2389 (0.2198–0.3052)	0.2615 (0.2117–0.3108)	0.1759 (0.1416–0.2083)	0.2237 (0.2202–0.2374)	0.3342 (0.2776–0.3969)	0.3669 (0.2876–0.3984)	0.3504 (0.2770–0.3974)	0.1713 (0.1373–0.2015)	0.1661 (0.1393–0.2052)
LAImaxIntcptn†	3	3	3	3	3	3	3	3	3	3	3	3
cVPD†	5	5	5	5	5	5	5	5	5	5	5	5
alphaCx#	0.0289 (0.0252–0.0383)	0.0400 (0.0286–0.0607)	0.0298 (0.0253–0.0376)	0.0367 (0.0316–0.0437)	0.0265 (0.0251–0.0317)	0.0567 (0.0456–0.0684)	0.0270 (0.0251–0.0301)	0.0285 (0.0251–0.0443)	0.0257 (0.0250–0.0283)	0.0653 (0.0573–0.0697)	0.0409 (0.0308–0.0525)	0.0406 (0.0313–0.0521)
Y†	0.47	0.47	0.47	0.47	0.47	0.47	0.47	0.47	0.47	0.47	0.47	0.47
MinCond†	0	0	0	0	0	0	0	0	0	0	0	0
MaxCond#	0.0137 (0.0102–0.0238)	0.0220 (0.0174–0.0239)	0.0210 (0.0163–0.0238)	0.0175 (0.0171–0.0192)	0.0235 (0.0138–0.0328)	0.0202 (0.0107–0.0287)	0.0246 (0.0244–0.0250)	0.0206 (0.0104–0.0343)	0.0178 (0.0149–0.0184)	0.0233 (0.0205–0.0265)	0.0250 (0.0194–0.0281)	0.0171 (0.0161–0.0221)
LAIgcx†	3.33	3.33	3.33	3.33	3.33	3.33	3.33	3.33	3.33	3.33	3.33	3.33
CoeffCond#	0.0889 (0.0768–0.0995)	0.0456 (0.0372–0.0546)	0.0522 (0.0426–0.0627)	0.0511 (0.0422–0.0618)	0.0573 (0.0438–0.0635)	0.0839 (0.0755–0.0986)	0.0896 (0.0780–0.0988)	0.0800 (0.0284–0.0991)	0.0825 (0.0633–0.0908)	0.0533 (0.0426–0.0622)	0.0473 (0.0392–0.0576)	0.0471 (0.0380–0.0559)
BLcond†	0.2	0.2	0.2	0.2	0.2	0.2	0.2	0.2	0.2	0.2	0.2	0.2
RGcGw†	0.66	0.66	0.66	0.66	0.66	0.66	0.66	0.66	0.66	0.66	0.66	0.66

Table 4 (continued)

Parameter	Abies alba	Acer pseudoplatanus	Betula	Fagus sylvatica	Fraxinus excelsior	Larix decidua	Picea abies	Pinus cembra	Pinus sylvestris	Pseudotsuga menziesii	Quercus petraea	Quercus robur
D13CTissueDif[†]	2	2	2	2	2	2	2	2	2	2	2	2
aFracDiffu[†]	4.4	4.4	4.4	4.4	4.4	4.4	4.4	4.4	4.4	4.4	4.4	4.4
bFracRubi[†]	27	27	27	27	27	27	27	27	27	27	27	27
fracBB0	0	0	0	0	0	0	0	0	0	0	0	0
fracBB1	0	0	0	0	0	0	0	0	0	0	0	0
tBB	0	0	0	0	0	0	0	0	0	0	0	0
rhoMin*	0.37	0.55	0.58	0.57	0.59	0.5	0.4	0.42	0.44	0.44	0.59	0.61
rhoMax*	0.37	0.55	0.58	0.57	0.59	0.5	0.4	0.42	0.44	0.44	0.59	0.61
tRho*	1	1	1	1	1	1	1	1	1	1	1	1
crownshape[†]	3	3	3	3	3	3	3	3	3	3	3	3
aH[‡]	30.91	30.66	20.09	30.42	35.5	40.17	37.73	43.7	45.69	46.09	39.46	36.34
nHB[‡]	16.78	14.36	6.42	11.65	13.99	19.84	17.85	29.1	23.01	24.57	16.37	14.15
nHC[‡]	0.00925	0.00513	0.01365	0.00825	0.00675	0.00398	0.00636	0	0.00576	0.00576	0	0.00148
aV[‡]	0.000128	0.000052	0.000049	0.000038	0.000054	0.000047	0.000115	0.000211	0.000118	0.000139	0.000031	0.000016
nVB[‡]	1.92	2.16	2.25	1.99	1.82	1.53	2.31	2.15	2.05	2.04	2	1.68
nVH[‡]	0.75	0.74	0.65	1.02	1.07	1.43	0.33	0.29	0.58	0.54	1.05	1.62
nVBH[‡]	0	0	0	0	0	0	0	0	0	0	0	0
aK[‡]	0.83	0.88	0.37	0.43	0.43	0.66	0.63	0.62	0.65	0.65	0.31	0.31
nKB[‡]	0.53	0.6	0.84	0.73	0.81	0.72	0.64	0.7	0.83	0.69	1.03	1.01
nKH[‡]	0	0	0	0	0	0	0	0	0	0	0	0
nKC[‡]	0	0	0	0.122	0	-0.14	-0.069	-0.196	-0.267	-0.037	-0.15	-0.111
nKrh[‡]	0	0	0	-0.126	0	0.248	0.067	-0.354	-0.087	0.196	0	0
aHL[‡]	24.93	18.42	9.72	23.32	17.23	27.97	35.18	18.07	11.77	21.18	20.13	23.41
nHLB[‡]	25.09	19.35	6.35	14.95	13.92	28.73	27.18	26.58	17.01	24.73	19.05	19.75
nHLL[‡]	0	0	0	0	0	0	0	0	0	0	0	0
nHLC[‡]	-0.002	0	0.005	0	0	-0.002	-0.005	0	0	0.002	0	-0.003
nHLrh[‡]	0	0	0	0	0	0	0	0	0	0	0	0
Dscale0[‡]	-2.052	-2.668	-3.612	-2.439	-2.429	-1.624	-2.023	-1.981	-1.049	-1.568	-0.861	-0.129
DscaleB[‡]	1.077	2.081	2.043	1.008	1.308	1.235	1.136	0.271	0.801	1.982	0.958	1.44
Dscalerh[‡]	0.757	0.676	0	0.21	0	0	0.051	0.171	0	0.055	0	0
Dscalet[‡]	0	0.04	0	0.187	0	-0.237	-0.049	0.46	0.108	-0.902	0	0
DscaleC[‡]	0.403	-0.328	0	0.295	0.199	0.435	0.382	0.608	0.186	0.395	0	-0.748
Dshape0[‡]	-0.13	-3.434	0.508	0.491	0.475	-0.109	0.328	-0.293	-0.689	0.985	-0.792	-0.34
DshapeB[‡]	0.228	1.882	0	0.345	0	0.481	0.562	0	0.372	0	0	0.764
Dshaperh[‡]	0.777	3.007	0	0.701	0	0.639	0.037	0	0	0	0	0
Dshapet[‡]	0	0	0	-0.138	0	-0.195	-0.254	0.426	0	-0.073	0.583	-0.287
DshapeC[‡]	0	0	0	-0.128	0	0	-0.117	0.426	0.111	-0.073	0.583	0
Dlocation0[‡]	0.462	1.485	2.167	0.723	0.601	0.293	0.391	0.652	0.129	0.284	-0.444	0.572

Table 4 (continued)

Parameter	Abies alba	Acer pseudoplatanus	Betula	Fagus sylvatica	Fraxinus excelsior	Larix decidua	Picea abies	Pinus cembra	Pinus sylvestris	Pseudotsuga menziesii	Quercus petraea	Quercus robur
DlocationB[‡]	0.825	0.266	0	0.87	0.646	0.874	0.847	1.867	1.057	−0.241	1.014	0.61
Dlocationrh[‡]	0	0	0	0	0	0	−0.004	−0.143	0	0.065	0	0
Dlocationt[‡]	0	0	0	−0.138	0	0	−0.001	−0.662	−0.158	0.944	0	0
DlocationC[‡]	−0.2	0	0	−0.111	0	−0.224	−0.187	−0.455	−0.103	−0.152	0	0
wsscale0[‡]	−3.118	−3.475	−2.852	−3.508	−3.513	−2.768	−3.366	−3.531	−2.905	−3.454	−2.438	−2.19
wsscaleB[‡]	2.384	2.715	2.619	2.445	2.859	2.461	2.369	1.794	2.081	2.447	2.606	2.696
wsscalerh[‡]	1.255	1.183	3.294	0.401	0	0.114	0.222	0	0	0.118	0	0
wsscalet[‡]	0	0	0	0.174	0	−0.192	−0.033	0.294	−0.026	0	0	0
wsscaleC[‡]	0.353	0.206	0	0.155	0.143	0.239	0.402	0.698	0.671	0.572	0	0
wsshape0[‡]	0.46	0.247	−2.162	0.551	1.481	−0.491	0.16	−0.242	−0.404	0.323	−1.287	0.427
wsshapeB[‡]	0.107	0	0.885	0.288	0.297	0.489	0.461	0	0.405	1.369	0.553	0
wsshaperh[‡]	0.705	0	0	0.585	0	0.428	0.273	0	0	0	0	0
wsshapet[‡]	0	0	0	−0.158	−0.537	−0.19	−0.241	0	−0.098	−1.263	0	0
wsshapeC[‡]	−0.196	0	0	−0.188	0\	0	−0.085	0.265	0	0	0	0
wslocation0[‡]	−0.168	1.902	1.459	−0.081	1.257	−1.092	−0.937	−0.825	−2.999	−0.854	−0.966	−1.125
wslocationB[‡]	1.555	0.487	0	1.915	2.311	1.88	2.005	4.113	2.564	−0.126	1.651	1.979
wslocationrh[‡]	0	−0.381	−1.164	−0.795	−2.136	0	−0.735	−0.68	−1.081	0.112	0	0
wslocationt[‡]	0	0	0	−0.483	−0.934	0	−0.228	−1.405	−0.387	1.971	0	0
wslocationC[‡]	−0.282	0	0.894	0.1	0	−0.469	−0.194	−0.858	0.291	−0.609	0	0
Qa[†]	−90	−90	−90	−90	−90	−90	−90	−90	−90	−90	−90	−90
Qb[†]	0.8	0.8	0.8	0.8	0.8	0.8	0.8	0.8	0.8	0.8	0.8	0.8
gDM_mol[†]	24	24	24	24	24	24	24	24	24	24	24	24
molPAR_MJ[†]	2.3	2.3	2.3	2.3	2.3	2.3	2.3	2.3	2.3	2.3	2.3	2.3

parameter distributions based only on the calibration plots (Step 2), measured by the 95% quantile range (see Table 5), was on average only 69% of the width of the prior ranges (which are shown in Tables 2 and 5). This was reduced to 63% when considering the posterior parameter distributions based on the calibration and validation plots (Step 4) (Table 5). This reduction in the uncertainty of the parameters was greater for more common species (e.g. 20% for *P. abies*) than for rarer species in the data set (e.g. 81–82% for *F. excelsior* and *P. cembra*) (Table 5). The largest reduction in uncertainty for all species was for parameters associated with biomass partitioning (pFS20), root or foliage litterfall (gammaF1, gammaR) and light-use efficiency (alphaCx), while the lowest reduction in uncertainty was for parameters defining the responses to vapour pressure deficit, temperature or CO_2 (CoeffCond, Tmax, fCg700) and the canopy interception of precipitation (MaxIntcptn).

3-PG model evaluation and validation for monocultures

3-PG reliably predicted the biomass stocks of the monospecific plots used for validation. The pBias was generally less than 20%, for stems, foliage and roots, and for several species it was less than 10% (*L. decidua, P. menziesii* and *Q. robur*) (Fig. 2). In comparison, the pBias for the calibration plots was generally < 10%, except for species with sample sizes that were too low to do a validation (*B. pendula, A. pseudoplatanus, F. excelsior, P. cembra*) (Fig. 2). As expected, the RMSE was highest for stem mass because this stock is typically much greater than root or foliage biomass. After accounting for differences in the size of stem stocks compared with root and foliage stocks, the NRMSE indicated that the foliage mass predictions had the highest errors.

3-PG model evaluation and validation for mixtures

The parameters resulted in accurate predictions for mixed-species plots in terms of stem, foliage (not shown) and root biomass, as well as other outputs derived from them such as *d*, height and basal area (Fig. 3). The slopes of the relationships between the predicted and observed values were usually close to 1 and not significantly different to 1. The exceptions included *A. alba*, which often also had a high pBias, and *P. abies* in terms of stem and root mass (Fig. 3; Table 6).

Discussion

For all twelve European tree species, the Bayesian calibration provided parameter sets with prediction bias < 20% and in several cases < 10%. Given the wide range of site, climate and stand structural conditions covered by the plots of many of these species, the parameters are expected to be generally applicable for central European forests. Similarly, 3-PG parameters for species in North America, South America and Thailand, developed from a sample of plots within a population, have been successfully applied across wide ranges of site conditions and management (Almeida et al. 2010; Gonzalez-Benecke et al. 2014, 2016; Hung et al. 2016; Thomas et al. 2017). Consistent with this study, Bayesian calibrations using outputs including basal area, volume, biomass stocks, mean tree diameter or height, tree and soil nutrition, leaf area index and net primary productivity have produced accurate predictions for other process-based forest models (Minunno et al. 2019; van Oijen et al. 2013, 2005).

The reduction in parametric uncertainty was often larger for the parameters to which output variables of 3-PG have been found to be highly sensitive (e.g. alphaCx, pFS20, gammaF1), and minimal to parameters to which 3-PG outputs are relatively insensitive (e.g. Tmax, CoeffCond, MaxIntcptn) (for 3-PG sensitivity analyses, see Almeida et al. 2004; Esprey et al. 2004; Forrester and Tang 2016; Law et al. 2000; Mathys et al. 2014; Meyer et al. 2017; Navarro-Cerrillo et al. 2016; Pérez-Cruzado et al. 2011; Potithep and Yasuoka 2011; Xenakis et al. 2008). The largest reduction in uncertainty for all species was for parameters associated with biomass partitioning (pFS20), root or foliage litterfall (gammaF1, gammaR) and light-use efficiency (alphaCx). The gammaR is only used to calculate the loss of root mass and has no influence on other variables, which explains why it was so easily constrained by the output variable root mass. The pFS20 (and pFS2) controls the partitioning of above-ground biomass growth between stems and foliage, and the gammaF1 controls the foliage litterfall rate. These are therefore important determinants of two output variables that we used to constrain 3-PG (stem mass and foliage mass). They are also important determinants of stand structure (e.g. leaf area index, mean tree size) and hence processes including light absorption and mortality. Similarly, for several species there was a high reduction in uncertainty in the light extinction parameter (k) and the potential light-use efficiency parameter (alphaCx), which are also very influential parameters in terms of biomass production. Parametric uncertainty was improved very little for Tmax, CoeffCond and MaxIntcptn. The former two parameters were also not improved in another study using inverse modelling with 3-PG, despite including Eddy covariance evapotranspiration data to constrain the model (Thomas et al. 2017). Therefore, reductions in parametric uncertainty appear to be higher for parameters to which the model is most sensitive as well as parameters that influence the output variables used for the inverse modelling.

Inter-specific differences in parameters often confirmed expected inter-specific differences in physiology.

Table 5 Posterior parameter ranges as percentages of the prior parameter ranges. The prior range is 95% of the estimated range between which the parameter for the given species can occur (Table 2), which was based on the literature review (Table S12). The posterior ranges are narrower ranges produced by the Bayesian calibration based on the "observed" biomass of the plots. The percentages are shown for two sets of posterior ranges. The first set were obtained from Bayesian calibration with only the calibration plots (Step 2: posterior ranges shown in Table 3). The second set are based on Bayesian calibration using all calibration and validation plots (Step 4: posterior ranges shown in Table 4)
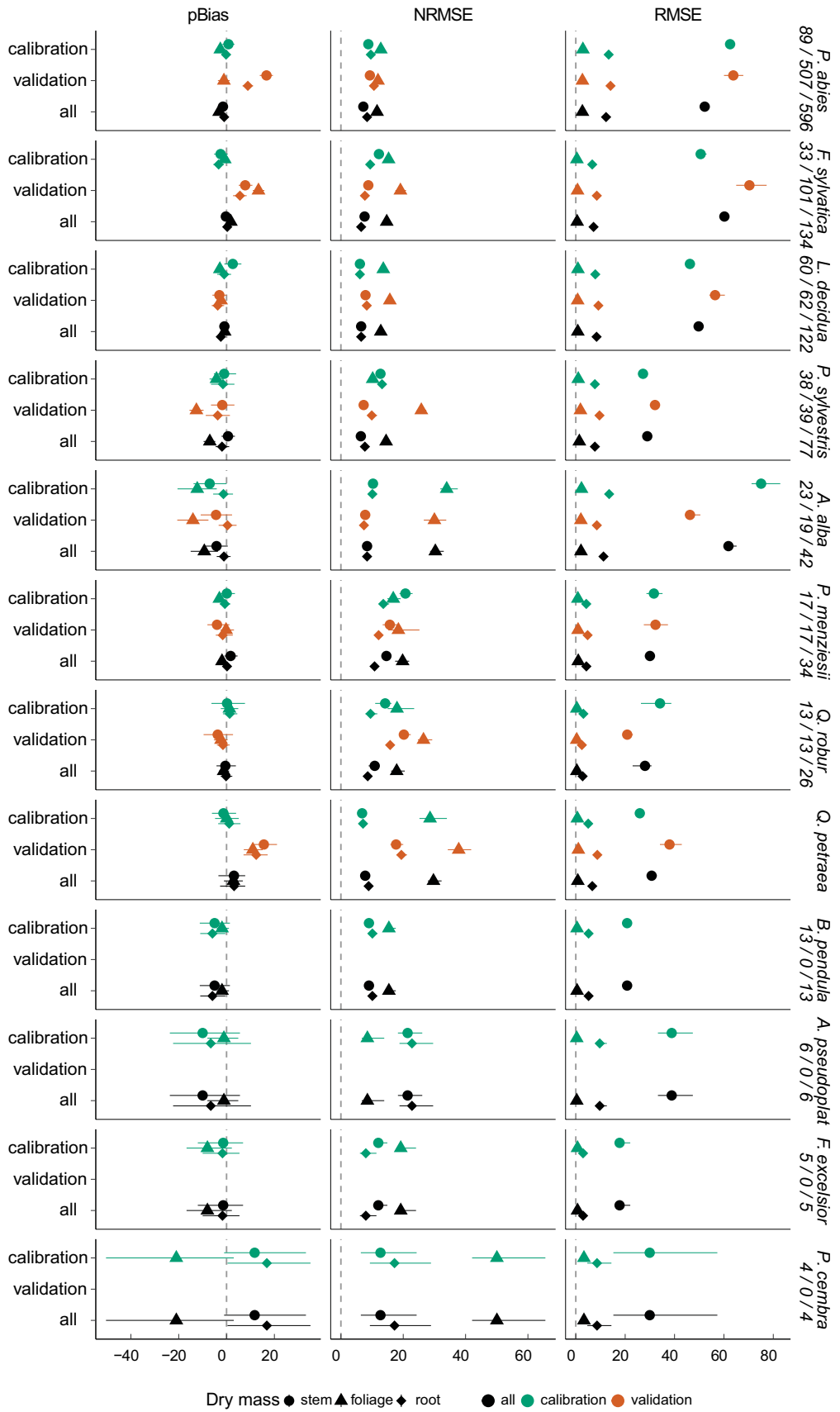
Parameter	Abies alba	Acer pseudoplatanus	Betula pendula	Fagus sylvatica	Fraxinus excelsior	Larix decidua	Picea abies	Pinus cembra	Pinus sylvestris	Pseudotsuga menziesii	Quercus petraea	Quercus robur	Mean for all species
Percentages calculated using posterior ranges based on only the calibration plots													
pFS2	92	86	90	3	97	71	50	88	11	6	85	6	57
pFS20	28	4	3	0	13	1	5	93	7	12	2	1	14
pRx	98	96	99	97	93	100	81	92	86	37	86	96	88
pRn	69	96	76	28	95	33	44	94	91	30	74	30	63
gammaF1	79						7	57	4	49			39
gammaR	0	9	0	1	1	0	0	1	2	0	2	1	2
Tmin	99	96	84	26	100	65	6	87	98	72	100	100	78
Topt	98	96	97	36	99	65	8	82	96	57	97	101	78
Tmax	100	99	101	96	100	100	16	99	99	99	100	100	92
fCalpha700	100	100	99	95	100	71	15	100	65	99	95	96	86
fCg700	99	99	100	96	100	99	64	100	96	98	89	100	95
wSx1000	63	100	99	97	101	99	30	72	38	53	41	16	67
thinPower	49	100	99	98	100	98	57	63	79	83	70	9	75
k	97	98	84	56	99	14	100	98	101	58	62	66	78
MaxIntcptn	100	99	101	94	100	100	42	100	97	98	99	100	94
alphaCx	30	75	29	39	15	46	33	45	10	41	51	47	38
MaxCond	76	86	99	36	80	57	14	101	69	80	96	101	75
CoeffCond	98	100	100	94	97	98	96	93	97	99	101	100	98
Mean for all parameters	76	85	80	58	82	66	37	81	64	59	73	63	69
Percentages calculated using posterior ranges based on calibration and validation plots													
pFS2	81	86	90	3	97	75	27	88	35	4	74	3	55
pFS20	20	4	3	0	13	1	4	93	5	8	2	1	13
pRx	98	96	99	95	93	97	51	92	75	34	87	88	84
pRn	52	96	76	21	95	28	26	94	92	23	73	29	59
gammaF1	72						2	57	3	33			33
gammaR	0	9	0	0	1	0	0	1	1	0	1	1	1
Tmin	96	96	84	22	100	44	2	87	97	32	94	100	71
Topt	94	96	97	33	99	57	3	82	92	36	85	101	73
Tmax	100	99	101	96	100	100	6	99	99	96	100	101	92
fCalpha700	100	100	99	13	100	93	5	100	31	98	84	82	75
fCg700	101	99	100	52	100	99	36	100	77	96	78	98	86

Table 5 (continued)

Parameter	Abies alba	Acer pseudoplatanus	Betula pendula	Fagus sylvatica	Fraxinus excelsior	Larix decidua	Picea abies	Pinus cembra	Pinus sylvestris	Pseudotsuga menziesii	Quercus petraea	Quercus robur	Mean for all species
wSx1000	54	100	99	64	101	100	20	72	19	14	45	18	59
thinPower	43	100	99	50	100	62	34	63	47	40	80	9	61
k	55	98 s	84	37	99	40	17	98	46	42	64	50	61
MaxIntcptn	100	99	101	82	100	100	16	100	92	95	100	100	90
alphaCx	31	75	29	28	15	53	12	45	8	29	51	49	35
MaxCond	57	86	99	26	80	76	6	101	60	71	97	79	70
CoeffCond	100	100	100	99	97	98	92	93	95	98	100	100	98
Mean for all parameters	70	85	80	42	82	66	20	81	54	47	71	59	63

For example, the potential light-use efficiency parameter (alphaCx) was highest for species known to have potentially high growth rates (e.g. *P. menziesii, L. decidua*) and intermediate for species such as *F. sylvatica* and *Q. robur/Q. petraea*. Nevertheless, it is important to note that the inverse modelling approach only provides an indirect indication of the parameters in terms of their physiological and ecological meanings.

In general, species for which the parametric uncertainty was reduced the most were those with the highest sample sizes. However, the prediction bias did not always decline with increasing numbers of plots, such that some of the most abundant species in the data set (e.g. *F. sylvatica, P. abies* and *P. sylvestris*) had prediction errors of > 10%, at least for some variables. Given that the accuracy of 3-PG predictions can be improved by developing different parameter sets for different provenances or even for different clones (Almeida et al. 2004), the larger prediction errors may have resulted from a greater intra-specific genetic diversity within the populations of these species. For example, *P. sylvestris* has a large physiological and morphological plasticity (Rehfeldt et al. 2002), and our data set included several provenance trials, although none were abundant enough to develop provenance-specific parameter sets.

A parameterization of the BGC forest model for *P. abies* indicated that different parameter sets were required for populations at low and high elevations (means of 607 m vs. 1385 m) (Pietsch et al. 2005). We did not observe any elevation-related effect on the bias of *P. abies* predictions and used a single parameter set for all elevations (282–2065 m). A single parameter set was also found to be appropriate in Finnish *P. abies* parameterizations of the PREBAS model (Minunno et al. 2019). This may indicate that 3-PG and PREBAS account for a cause of the elevation differences that was not accounted for by the BGC model.

Since all models are simplifications of reality, they inevitably do not include all the processes that influence their outputs. Consequently, some of the parameters within the model may compensate for missing information, and as a result, they will not represent exactly what is implied by their parameter name (van Oijen 2017). Preliminary calibrations showed that the self-thinning parameter (w_{Sx1000}) required different values than indicated by the means of many published values, and the prior ranges therefore needed to be widened. Self-thinning parameters were also required to vary between experiments for Bayesian calibrations of 3-PG for *Pinus taeda* (Thomas et al. 2017). This may indicate that improvements can be made to 3-PG in relation to quantifying the carrying capacity of a site, although the effects of site and climate on self-thinning rates do not appear large enough in Swiss forests to account for this (Forrester et al. 2021). This also indicates the value of validating each sub-model by comparing predicted outputs

◄**Fig. 2** Statistics for predictive error (percent bias, normalized root mean squared error and root mean squared error). The posterior predictive uncertainty was calculated by drawing 1,000 parameter combinations from the posteriori distribution and calculating model predictions for the calibration (green dots), validation (orange dots) and calibration+validation (black dots) monitoring data subsets. The dots represent the median value of the posterior predictive distribution, while the horizontal lines represent the 95% confidence interval. Species are ordered by number of available monitoring plots for calibration and validation. Numbers under the species name indicate the number of monitoring plots used for calibration and validation. For *B. pendula, A. pseudoplatanus, F. excelsior, P. cembra*, the samples sizes were too small to do a validation

from the given sub-model with measurements of the same process, rather than indirect approaches that, for example, validate a light or water balance sub-model using growth and yield data (Korzukhin et al. 1996; Sands 2004). This provides confidence that the sub-models perform as their names imply and therefore that deviations in parameter estimates based on Bayesian calibrations, compared with field measurements of the parameters, are likely to indicate a missing process within the model, rather than significant problems with existing model components.

Another source of error is the calculation of biomass. The "observed" biomass was predicted using allometric equations developed from an independent European-wide data set (Forrester et al. 2017b). However, even though these equations accounted for variables such as tree diameter and stand density, they are unlikely to be as accurate as site-specific destructively sampled biomass measurements, and they will not reflect the short-term (monthly or annual) variability in biomass allocation that is predicted by 3-PG. In this study, we did not account for the errors associated with the allometric biomass equations or the allometric equations used to obtain 3-PG parameters for height, crown length and crown diameter. Therefore, the ranges of the parameter posterior distributions may have been underestimated, and when estimates of errors are required when forecasting, the variance related to the allometric equations would need to be considered in the outputs.

By setting the soil fertility for all plots to 0.5, some of the other parameters would have been forced to account for variability in biomass that was actually due to soil fertility. The resulting influence of this approach on the parameter estimates is assumed to be relatively low because of the large number of plots used and because many of the plots are

Fig. 3 Comparison of observed and predicted stem biomass (**a**), root biomass (**b**), arithmetic mean diameter (**c**) and mean height (**d**) for a selection of 6 species in 13 mixed-species plots. Note that the "observed" biomass was calculated using allometric biomass equations. Only data from the end of the simulations are shown; for a given species, only one point is shown for each plot where that species occurred at the end of the simulations. The solid lines are 1:1 lines, and the dashed lines are fitted to the data to pass through the origin. Sample size $N=24$
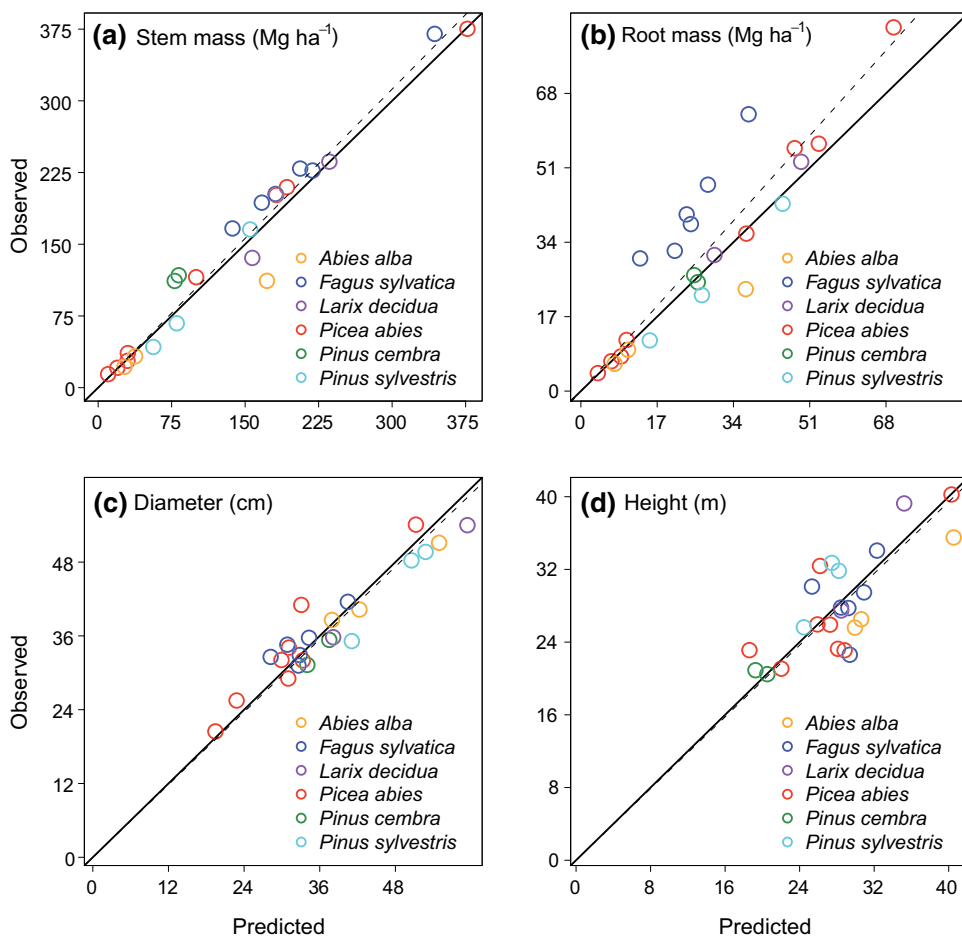
Table 6 Statistical information that describes the relationships between the predicted and observed variables for mixtures as shown in Fig. 3. The statistical information includes the percentage bias (pBias%), the relative mean absolute error (MAE%), the slope of the relationship forced through the origin, the *P*-value for the test of whether the slope of the relationship is significantly different from 1, and the R^2 values. The mean species proportion is in terms of the contribution made to total stand basal area

Output variable	Species	pBias	Slope	*P*-value	R^2	Mean species proportion	Time-series length (years; and minimum/maximum)	Number of plots
Stem mass	*Picea abies*	4.6	0.95	0.003	0.999	0.44	27 (16/42)	8
Stem mass	*Pinus cembra*	− 14.1	1.16	0.131	0.999	0.3	42 (42/42)	2
Stem mass	*Pinus sylvestris*	4.8	0.98	0.755	0.994	0.38	32 (17/47)	3
Stem mass	*Abies alba*	53.5	0.6	0.012	0.989	0.15	26 (22/35)	3
Stem mass	*Fagus sylvatica*	− 1.9	1.01	0.668	0.997	0.62	27 (16/47)	6
Stem mass	*Larix decidua*	2.7	0.97	0.178	1	0.63	20 (19/21)	2
Root mass	*Picea abies*	− 9.4	1.13	0.004	0.995	0.44	27 (16/42)	8
Root mass	*Pinus cembra*	− 0.1	1	0.994	0.998	0.3	42 (42/42)	2
Root mass	*Pinus sylvestris*	14.4	0.9	0.199	0.993	0.38	32 (17/47)	3
Root mass	*Abies alba*	40.5	0.66	0.024	0.987	0.15	26 (22/35)	3
Root mass	*Fagus sylvatica*	− 41.1	1.68	< 0.001	0.992	0.62	27 (16/47)	6
Root mass	*Larix decidua*	− 5.5	1.06	0.103	1	0.63	20 (19/21)	2
Mean diameter	*Picea abies*	− 6.1	1.06	0.093	0.993	0.44	27 (16/42)	8
Mean diameter	*Pinus cembra*	7.4	0.93	0.107	1	0.3	42 (42/42)	2
Mean diameter	*Pinus sylvestris*	8.5	0.93	0.118	0.998	0.38	32 (17/47)	3
Mean diameter	*Abies alba*	4	0.96	0.217	0.999	0.15	26 (22/35)	3
Mean diameter	*Fagus sylvatica*	− 4.4	1.04	0.188	0.996	0.62	27 (16/47)	6
Mean diameter	*Larix decidua*	8.7	0.92	0.103	1	0.63	20 (19/21)	2
Mean height	*Picea abies*	1	0.98	0.73	0.981	0.44	27 (16/42)	8
Mean height	*Pinus cembra*	− 3.8	1.04	0.542	0.998	0.3	42 (42/42)	2
Mean height	*Pinus sylvestris*	− 11.2	1.13	0.085	0.997	0.38	32 (17/47)	3
Mean height	*Abies alba*	15.4	0.87	0.002	1	0.15	26 (22/35)	3
Mean height	*Fagus sylvatica*	2.2	0.98	0.665	0.985	0.62	27 (16/47)	6
Mean height	*Larix decidua*	− 4.6	1.06	0.585	0.995	0.63	20 (19/21)	2

likely to have FR close to 0.5 assuming a roughly normal distribution of FR. However, the parameters could still be improved when reliable soil fertility information becomes available.

Lastly, the parameter sets generally provided accurate predictions for mixed-species forests. The validation for mixtures was based on small sample sizes (13 mixed-species plots) due to the difficulty in finding even-aged mixtures that only contained the species that had been parameterized. Nevertheless, these results confirm that 3-PG can be calibrated using monocultures and applied to mixtures, as previously found in Europe (Bouwman et al. 2021; Forrester et al. 2017a) and China (Forrester and Tang 2016).

In conclusion, the combination of a literature review, direct estimation of many allometric parameters, several inventory plot networks and Bayesian calibration resulted in reliable 3-PG parameters for twelve major European species. These parameters are also applicable for mixed-species forests. The information sources used to develop the parameters included a wide range of climatic, edaphic and management conditions and long time spans (from 1930 to present). Given this and the process-based structure of the 3-PG model, these parameters are likely to be applicable for most central European forests and conditions.

References

Almeida AC, Sands PJ, Bruce J, Siggins AW, Leriche A, Battaglia M, Batista TR (2009) Use of a spatial process-based model to quantify forest plantation productivity and water use efficiency under climate change scenarios. In: Anderssen RS, Braddock RD, Newham LTH (eds) Interfacing modelling and simulation with mathematical and computational sciences. Modelling and Simulation Society of Australia and New Zealand and International Association for Mathematics and Computers in Simulation, Cairns, Australia, pp 1816–1822

Almeida AC, Siggins A, Batista TR, Beadle C, Fonseca S, Loos R (2010) Mapping the effect of spatial and temporal variation in climate and soils on *Eucalyptus* plantation production with 3-PG, a process-based growth model. For Ecol Manag 259:1730–1740

Almeida ACd, Landsberg JJ, Sands PJ (2004) Parameterisation of 3-PG model for fast-growing *Eucalyptus grandis* plantations. For Ecol Manag 193:179–195

Augustynczik ALD, Hartig F, Minunno F, Kahle H-P, Diaconu D, Hanewinkel M, Yousefpour R (2017) Productivity of *Fagus sylvatica* under climate change - a Bayesian analysis of risk and uncertainty using the model 3-PG. For Ecol Manag 401:192–206

Bartoń K (2016) Multi-Model Inference, R Package 'MuMIn' version 1.15.6

Battaglia M, Sands P, White D, Mummery D (2004) CABALA: a linked carbon, water and nitrogen model of forest growth for silvicultural decision support. For Ecol Manag 193:251–282

Battaglia M, Sands PJ (1998) Process-based forest productivity models and their application in forest management. For Ecol Manag 102:13–32

Bouwman M, Forrester DI, Ouden Jd, Nabuurs G-J, Mohren GMJ (2021) Species interactions in mixed stands of *Pinus sylvestris* and *Quercus robur* in the Netherlands: competitive dominance shifts in favor of *P. sylvestris* under projected climate change. For Ecol Manag 481:118615

Coops NC, Waring RH (2011) Estimating the vulnerability of fifteen tree species under changing climate in Northwest North America. Ecol Model 222:2119–2129

Duursma RA, Medlyn BE (2012) MAESPA: a model to study interactions between water limitation, environmental drivers and vegetation function at tree and stand levels, with an example application to [CO_2] × drought interactions. Geosci Model Dev 5:919–940

Esprey LJ, Sands PJ, Smith CW (2004) Understanding 3-PG using a sensitivity analysis. For Ecol Manag 193:235–250

Fer I, Kelly R, Moorcroft PR, Richardson AD, Cowdery EM, Dietze MC (2018) Linking big models to big data: efficient ecosystem model calibration through Bayesian model emulation. Biogeosciences 15:5801–5830

Fischer C, Traub B (2019) Swiss national forest inventory – methods and models of the fourth assessment, managing forest ecosystems. Springer International Publishing, Cham

Fontes L, Bontemps JD, Bugmann H, van Oijen M, Gracia C, Kramer K, Lindner M, Rötzer T, Skovsgaard JP (2010) Models for supporting forest management in a changing environment. For Syst 19:8–29

Forrester DI (2020) 3-PG User Manual (available from https://sites.google.com/site/davidforresterssite/home/projects/3PGmix/3pgmixdownload). Swiss Federal Institute for Forest, Snow and Landscape Research WSL, Birmensdorf, Switzerland, p 70

Forrester DI, Ammer C, Annighöfer PJ, Avdagic A, Barbeito I, Bielak K, Brazaitis G, Coll L, Río Md, Drössler L, Heym M, Hurt V, Löf M, Matović B, Meloni F, Ouden Jd, Pach M, Pereira MG, Ponette Q, Pretzsch H, Skrzyszewski J, Stojanović D, Svoboda M, Ruiz-Peinado R, Vacchiano G, Verheyen K, Zlatanov T, Bravo-Oviedo A (2017) Predicting the spatial and temporal dynamics of species interactions in *Fagus sylvatica* and *Pinus sylvestris* forests across Europe. For Ecol Manag 405:112–133

Forrester DI, Baker TG, Elms SR, Hobi ML, Ouyang S, Wiedemann JC, Xiang W, Zell J, Pulkkinen M (2021) Self-thinning tree mortality models that account for vertical stand structure, species mixing and climate. For Ecol Manag 487:118936

Forrester DI, Guisasola R, Tang X, Albrecht AT, Dong TL, le Maire G (2014) Using a stand-level model to predict light absorption in stands with vertically and horizontally heterogeneous canopies. For Ecosyst 1:17

Forrester DI, Nitzsche J, Schmid H (2019) The Experimental Forest Management project: An overview and methodology of the long-term growth and yield plot network. Swiss Federal Institute of Forest, Snow and Landscape Research WSL. Available from https://www.wsl.ch/en/projects/long-term-growth-and-yield-data.html, p 77

Forrester DI, Tachauer IHH, Annighoefer P, Barbeito I, Pretzsch H, Ruiz-Peinado R, Stark H, Vacchiano G, Zlatanov T, Chakraborty T, Saha S, Sileshi GW (2017b) Generalized biomass and leaf area allometric equations for European tree species incorporating stand structure, tree age and climate. For Ecol Manag 396:160–175

Forrester DI, Tang X (2016) Analysing the spatial and temporal dynamics of species interactions in mixed-species forests and the effects of stand density using the 3-PG model. Ecol Model 319:233–254

Gelman A, Rubin DB (1992) Inference from iterative simulation using multiple sequences. Stat Sci 7:457–472

Gertner GZ, Fang S, Skovsgaard JP (1999) A Bayesian approach for estimating the parameters of a forest process model based on long-term growth data. Ecol Model 119(2–3):249–265

Gonzalez-Benecke CA, Jokela EJ, Cropper WP Jr, Bracho R, Leduc DJ (2014) Parameterization of the 3-PG model for *Pinus elliottii* stands using alternative methods to estimate fertility rating, biomass partitioning and canopy closure. For Ecol Manag 327:55–75

Gonzalez-Benecke CA, Teskey RO, Martin TA, Jokela EJ, Fox TR, Kane MB, Noormets A (2016) Regional validation and improved parameterization of the 3-PG model for *Pinus taeda* stands. For Ecol Manag 361:237–256

Gupta R, Sharma LK (2019) The process-based forest growth model 3-PG for use in forest management: a review. Ecol Model 397:55–73

Hartig F, Dyke J, Hickler T, Higgins SI, O'Hara RB, Scheiter S, Huth A (2012) Connecting dynamic vegetation models to data – an inverse perspective. J Biogeogr 39:2240–2252

Hobi M, Stillhard J, Projer G, Mathys A, Bugmann H, Brang P (2020) Forest reserves monitoring in Switzerland. EnviDat. https://doi.org/10.16904/envidat.141

Hung TT, Almeida AC, Eyles A, Mohammed C (2016) Predicting productivity of *Acacia* hybrid plantations for a range of climates and soils in Vietnam. For Ecol Manag 367:97–111

Korzukhin MD, TerMikaelian MT, Wagner RG (1996) Process versus empirical models: which approach for forest ecosystem management? Can J For Res 26:879–887

Landsberg J, Mäkelä A, Sievänen R, Kukkola M (2005) Analysis of biomass accumulation and stem size distributions over long periods in managed stands of *Pinus sylvestris* in Finland using the 3-PG model. Tree Physiol 25:781–792

Landsberg J, Sands P (2011) The 3-PG process-based model. Physiological ecology of forest production: principles, processes and models. Elsevier, Amsterdam, pp 241–282

Landsberg JJ, Waring RH (1997) A generalised model of forest productivity using simplified concepts of radiation-use efficiency, carbon balance and partitioning. For Ecol Manag 95:209–228

Lange KL, Little RJA, Taylor JMG (1989) Robust statistical modeling using the t distribution. J Am Stat Assoc 84:881–896

Law BE, Waring RH, Anthoni PM, Aber JD (2000) Measurements of gross and net productivity and water vapor exchange of a Pinus ponderosa ecosystem, and an evaluation of two generalized models. Glob Change Biol 6:155–168

Mathys A, Coops NC, Waring RH (2014) Soil water availability effects on the distribution of 20 tree species in western North America. For Ecol Manag 313:144–152

Meyer G, Black A, Jassal RS, Nesic Z, Grant NJ, Spittlehouse DL, Fredeen AL, Christen A, Coops NC, Foord VN, Bowler R (2017) Measurements and simulations using the 3-PG model of the water balance and water use efficiency of a lodgepole pine stand following mountain pine beetle attack. For Ecol Manag 393:89–104

Michajlow J (1952) Mathematische Formulierung des Gesetzes für Wachstum und Zuwachs der Waldbäume und Bestände. Schweiz Z Forstw 103:368–380

Minunno F, Peltoniemi M, Härkönen S, Kalliokoski T, Makinen H, Mäkelä A (2019) Bayesian calibration of a carbon balance model PREBAS using data from permanent growth experiments and national forest inventory. For Ecol Manag 440:208–257

Monteith JL (1965) Evaporation and environment. In: Fogg GA (ed) The state and movement of water in living organisms. Symposia of the society for experimental biology, vol 19. Academic Press, London, pp 205–234

Navarro-Cerrillo RM, Jesús Beira JS, Xenakis G, Sánchez-Salguero R, Hernández-Clemente R (2016) Growth decline assessment in *Pinus sylvestris L.* and *Pinus nigra* Arnold forests by using 3-PG model. For Syst 25:e068

Panagos P, Liedekerke MV, Jones A, Montanarella L (2012) European soil data centre: response to European policy support and public data requirements. Land Use Policy 29:329–338

Penman HL (1948) Natural evaporation from open water, bare soil and grass. Proc R Soc Lond (A) 193:120–145

Pérez-Cruzado C, Muñoz-Sáez F, Basurco F, Riesco G, Rodríguez-Soalleiro R (2011) Combining empirical models and the process-based model 3-PG to predict *Eucalyptus nitens* plantations growth in Spain. For Ecol Manag 262:1067–1077

Pietsch SA, Hasenauer H, Thornton PE (2005) BGC-model parameters for tree species growing in central European forests. For Ecol Manag 211:264–295

Pinheiro J, Bates D, DebRoy S, Sarkar D, R Core Team (2018) nlme: Linear and Nonlinear Mixed Effects Models. R package version 3.1–137

Potithep S, Yasuoka Y (2011) Application of the 3-PG model for gross primary productivity estimation in deciduous broadleaf forests: a study area in Japan. Forests 2:590–609

Pretzsch H, Forrester DI, Rötzer T (2015) Representation of species mixing in forest growth models. Rev Perspect Ecol Model 313:276–292

R Core Team (2019) R: A language and environment for statistical computing. R Foundation for Statistical Computing, Vienna, Austria. URL http://www.R-project.org/.

Rehfeldt GE, Tchebakova NM, Parfenova YI, Wykoff WR, Kuzmina NA, Milyutin LI (2002) Intraspecific responses to climate in *Pinus sylvestris*. Glob Change Biol 8:912–929

Sands P (2004) Adaptation of 3-PG to novel species: guidelines for data collection and parameter assignment. Technical Report No.141. CRC for Sustainable Production Forestry, (p 35)

Sands PJ, Landsberg JJ (2002) Parameterisation of 3-PG for plantation grown *Eucalyptus globulus*. For Ecol Manag 163:273–292

ter Braak CJF, Vrugt JA (2008) Differential evolution markov chain with snooker updater and fewer chains. Stat Comput 18:435–446

Thomas RQ, Brooks EB, Jersild AL, Ward EJ, Wynne RH, Albaugh TJ, Dinon-Aldridge H, Burkhart HE, Domec J-C, Fox TR, Gonzalez-Benecke CA, Martin TA, Noormets A, Sampson DA, Teskey RO (2017) Leveraging 35 years of Pinus taeda research in the southeastern US to constrain forest carbon cycle predictions: regional data assimilation using ecosystem experiments. Biogeosciences 14:3525–3547

Thornton PE, Running SW, White MA (1997) Generating surfaces of daily meteorological variables over large regions of complex terrain. J Hydrol 190:214–251

Trotsiuk V, Hartig F, Forrester DI (2020) r3PG – an R package for simulating forest growth using the 3-PG process-based model. Methods Ecol Evol 11:1470–1475

van Oijen M (2017) Bayesian methods for quantifying and reducing uncertainty and error in forest models. Curr For Rep 3:269–280

van Oijen M, Reyer C, Bohn FJ, Cameron DR, Deckmyn G, Flechsig M, Härkönen S, Hartig F, Huth A, Kiviste A, Lasch P, Mäkelä A, Mette T, Minunno F, Rammer W (2013) Bayesian calibration, comparison and averaging of six forest models, using data from Scots pine stands across Europe. For Ecol Manag 289:255–268

van Oijen M, Rougier J, Smith R (2005) Bayesian calibration of process-based forest models: bridging the gap between models and data. Tree Physiol 25:915–927

Vanclay JK, Skovsgaard JP (1997) Evaluating forest growth models. Ecol Model 98:1–12

Waring RH, Landsberg JJ, Williams M (1998) Net primary production of forests: a constant fraction of gross primary production. Tree Physiol 18:129–134

Wei L, Marshall JD, Link TE, Kavanagh KL, Du E, Pangle RE, Gag PJ, Ubierna N (2014) Constraining 3-PG with a new $\delta^{13}C$ submodel: a test using the $\delta^{13}C$ of tree rings. Plant Cell Environ 37:82–100

WSL (2020) Schweizerisches Landesforstinventar LFI, Daten der Erhebungen 1983/85 (LFI1), 1993/95 (LFI2), 2004/06 (LFI3) und 2009/17 (LFI4). Golo Stadelmann 15.04.2020. Eidg. Forschungsanstalt WSL, Birmensdorf

Xenakis G, Ray D, Mencuccini M (2008) Sensitivity and uncertainty analysis from a coupled 3-PG and soil organic matter decomposition model. Ecol Model 219:1–16

Yoda K, Kira T, Ogawa H, Hozami K (1963) Self thinning in overcrowded pure stands under cultivated and natural conditions. J Biol Osaka City Uni 14:107–129